CHAPTER 11

Flow in Open Channels

Case Study

Many flows of liquids in engineering and in nature occur with a free surface. An example of a human-made channel that carries water is shown in the photograph. This is a view of the 190-mile-long Hayden-Rhodes Aqueduct, which is part of the Central Arizona Project (CAP). The CAP is a 336-mile (541 km) diversion canal used to redirect water from the Colorado River into central and southern Arizona. The CAP originates in Lake Havasu on the western border of Arizona, travels through the Phoenix area, and terminates in the San Xavier Indian Reservation southwest of Tucson. It is designed to carry about 1.5 million acre-feet of Colorado River water per year, making it the largest single resource of renewable water supplies in the state of Arizona.

The design of the CAP involved many of the engineering principles we will study in this chapter. Because of the large flow rate of water, the aqueduct was designed as an open channel with a trapezoidal cross section that provided the smallest channel for the desired flow rate. Gravity is the driving force for the flow, and the land was graded to give the correct slope to the channel for the flow. As Lake Havasu is nearly 3000 feet below the terminus, the final aqueduct design included 15 pumping stations, 8 inverted siphons, and 3 tunnels.

Aqueduct, Central Arizona Project.

Free surface flows differ in several important respects from the flows in closed conduits that we studied in Chapter 8. Familiar examples where the free surface of a water flow is at atmospheric pressure include flows in rivers, aqueducts, irrigation canals, rooftop or street gutters, and drainage ditches. Human-made channels, termed aqueducts, encompass many different types, such as canals, flumes, and culverts. A canal usually is below ground level and may be unlined or lined. Canals generally are long and of very mild slope; they are used to carry irrigation or storm water or for navigation. A flume usually is built above ground level to carry water across a depression. A culvert, which usually is designed to flow only part-full, is a short covered channel used to drain water under a highway or railroad embankment.

Figure 11.1 illustrates a typical example of water flowing in an open channel. The channel, often called an aqueduct, carries water from a source, such as a lake, across the Earth's surface to where the

Fig. 11.1 A typical example of an open-channel flow of water; located in California's Central Valley with supply pipes visible in background.

water is needed, often for crop irrigation or as a water supply for a city. As you can see in this photograph, the channel is relatively wide with sloped sides and has a gradual slope that allows the water to proceed downhill. Water enters this aqueduct through large corrugated pipes from a higher elevation; the pipes are used because the slope of the hillside is too steep for an open channel. The structure at the entrance to the aqueduct could be a low head turbine that extracts power from the flowing water.

In this chapter we will introduce some of the basic concepts in open-channel flows. These flows are covered in much more detail in a number of specialized texts [1 – 8]. We will use the control volume concepts from Chapter 4 to develop the basic theory that describes the behavior and classification of flows in natural and human-made channels. We shall consider:

- *Flows for which the local effects of area change predominate and frictional forces may be neglected*. An example is flow over a bump or depression, over the short length of which friction is negligible.
- *Flow with an abrupt change in depth*. This occurs during a hydraulic jump in which the water flow goes from fast and shallow to slow and deep in a very short distance (see Fig 11.12).
- *Flow at what is called normal depth*. For this, the flow cross section does not vary in the flow direction; the liquid surface is parallel to the channel bed. This is analogous to fully developed flow in a pipe.
- *Gradually varied flow*. An example is flow in a channel in which the bed slope varies. The major objective in the analysis of gradually varied flow is to predict the shape of the free surface.

It is quite common to observe surface waves in flows with a free surface, the simplest example being when an object such as a pebble is thrown into the water. The propagation speed of a surface wave is analogous in many respects to the propagation of a sound wave in a compressible fluid medium (which we discuss in Chapter 12). We shall determine the factors that affect the speed of such surface waves. We will see that this is an important determinant in whether an open-channel flow is able to gradually adjust to changing conditions downstream or a hydraulic jump occurs.

This chapter also includes a brief discussion of flow measurement techniques for use in open channels.

11.1 *Basic Concepts and Definitions*

Before analyzing the different types of flows that may occur in an open channel, we will discuss some common concepts and state some simplifying assumptions. We are doing so explicitly, because there are some important differences between our previous studies of pipes and ducts in Chapter 8 and the study of open-channel flows.

One significant difference between flows in pipes and ducts is

- The driving force for open-channel flows is *gravity*.

(Note that some flows in pipes and ducts are also gravity driven (for example, flow down a full drainpipe), but typically flow is driven by a pressure difference generated by a device such as a pump.) The gravity force in open-channel flow is opposed by friction force on the solid boundaries of the channel.

Simplifying Assumptions

The flow in an open channel, especially in a natural one such as a river, is often very complex, three-dimensional, and unsteady. However, in most cases, we can obtain useful results by approximating such flows as being:

- *One-dimensional*.
- *Steady*.

A third simplifying assumption is:

- The flow at each section in an open-channel flow is approximated as a *uniform velocity*.

Although the actual velocity in a channel is really not uniform, we will justify this assumption. Figure 11.2 indicates the regions of the maximum velocity in some open-channel flow geometries. The minimum velocity is zero along the walls because of viscosity. Measurements show that the region of maximum velocity occurs below the free surface. There is a negligible shear stress due to air drag on the free surface, so one would expect the maximum velocity to occur at the free surface. However, secondary flows occur and produce a nonuniform velocity profile with the maximum usually occurring below the surface. Secondary flows also occur when a channel has a bend or curve or has an obstruction, such as a bridge pier. These obstructions can produce vortices that erode the bottom of a natural channel.

Most open-channel flows of water are large in physical scale, so the Reynolds number is generally quite high. Consequently, open-channel flow is seldom laminar, and so we will assume that the flow in open channels is always turbulent. As we saw in earlier chapters, turbulence tends to smooth out the velocity profile (see Fig. 8.11 for turbulent pipe flow and Fig. 9.7 for turbulent boundary layers). Hence, although there is a velocity profile in an open-channel flow, as indicated in Fig. 11.2, we will assume a uniform velocity at each section, as illustrated in Fig. 11.3a.

The next simplifying assumption we make is:

- The pressure distribution is approximated as *hydrostatic*.

This is illustrated in Fig. 11.3*b* and is a significant difference from the analysis of flows in pipes and ducts of Chapter 8; for these we found that the pressure was uniform at each axial location and varied in the streamwise direction. In open-channel flows, the free surface will be at atmospheric pressure (zero gage), so the pressure at the surface does not vary in the direction of flow. The major pressure variation occurs *across* each section; this will be exactly true if streamline curvature effects are negligible, which is often the case.

As in the case of turbulent flow in pipes, we must rely on empirical correlations to relate frictional effects to the average velocity of flow. The empirical correlation is included through a head loss term in the energy equation (Section 11.2). Additional complications in many practical cases include the

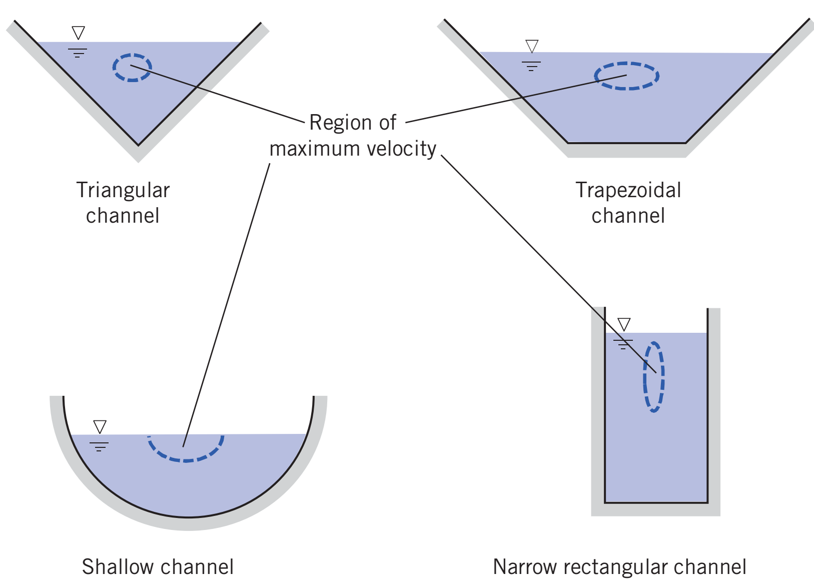

Fig. 11.2 Region of maximum velocity in some typical open-channel geometries. (Based on Chow [1].)

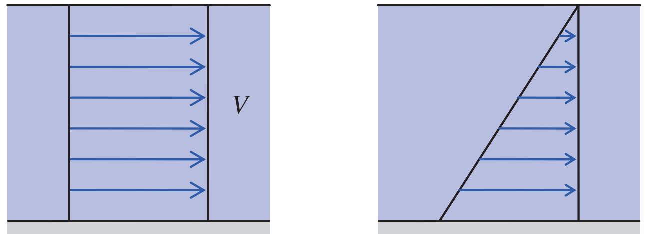

Fig. 11.3 Approximations for velocity profile and pressure distribution.

presence of sediment or other particulate matter in the flow, as well as the erosion of earthen channels or structures by water action.

Channel Geometry

Channels may be constructed in a variety of cross-sectional shapes; in many cases, regular geometric shapes are used. A channel with a constant slope and cross section is termed *prismatic*. Lined canals often are built with rectangular or trapezoidal sections; smaller troughs or ditches sometimes are triangular. Culverts and tunnels generally are circular or elliptical in section. Natural channels are highly irregular and nonprismatic, but often they are approximated using trapezoid or paraboloid sections. Geometric properties of common open-channel shapes are summarized in Table 11.1.

The *depth of flow*, y, is the perpendicular distance measured from the channel bed to the free surface. The *flow area*, A, is the cross section of the flow perpendicular to the flow direction. The *wetted perimeter*, P, is the length of the solid channel cross-sectional surface in contact with the liquid. The *hydraulic radius*, R_h, is defined as

$$R_h = \frac{A}{P} \tag{11.1}$$

For flow in noncircular closed conduits (Section 8.7), the hydraulic diameter was defined as

$$D_h = \frac{4A}{P} \tag{8.50}$$

Thus, for a circular pipe, the hydraulic diameter, from Eq. 8.50, is equal to the pipe diameter. From Eq. 11.1, the hydraulic radius for a circular pipe would then be *half* the actual pipe radius, which is a bit confusing! The hydraulic radius, as defined by Eq. 11.1, is commonly used in the analysis of open-channel flows, so it will be used throughout this chapter. One reason for this usage is that the hydraulic radius of a wide channel, as seen in Table 11.1, is equal to the actual depth.

For nonrectangular channels, the *hydraulic depth* is defined as

$$y_h = \frac{A}{b_s} \tag{11.2}$$

where b_s is the width at the surface. Hence the hydraulic depth represents the *average depth* of the channel at any cross section. It gives the *depth of an equivalent rectangular channel*.

Table 11.1
Geometric Properties of Common Open-Channel Shapes

Shape	Section	Flow Area, A	Wetted Perimeter, P	Hydraulic Radius, R_h
Trapezoidal	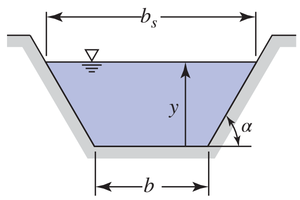	$y\,(b + y\cot\alpha)$	$b + \dfrac{2y}{\sin\alpha}$	$\dfrac{y\,(b + y\cot\alpha)}{b + \dfrac{2y}{\sin\alpha}}$
Triangular	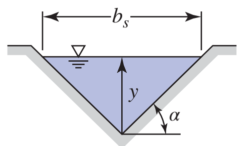	$y^2\cot\alpha$	$\dfrac{2y}{\sin\alpha}$	$\dfrac{y\cos\alpha}{2}$
Rectangular	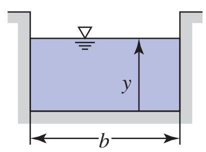	by	$b + 2y$	$\dfrac{by}{b + 2y}$
Wide Flat	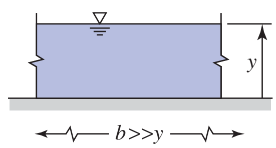	by	b	y
Circular	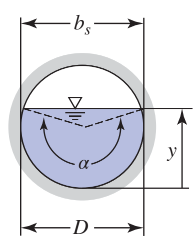	$(\alpha - \sin\alpha)\dfrac{D^2}{8}$	$\dfrac{\alpha D}{2}$	$\dfrac{D}{4}\left(1 - \dfrac{\sin\alpha}{\alpha}\right)$

Speed of Surface Waves and the Froude Number

We will learn later in this chapter that the behavior of an open-channel flow as it encounters downstream changes (for example, a bump of the bed surface, a narrowing of the channel, or a change in slope) is strongly dependent on whether the flow is "slow" or "fast." A slow flow will have time to gradually adjust to changes downstream, whereas a fast flow will also sometimes gradually adjust but in some situations will do so "violently" (i.e., there will be a hydraulic jump; see Fig. 11.12 for an example). The question is what constitutes a slow or fast flow? These vague descriptions will be made more precise now. It turns out that the speed at which surface waves travel along the surface is key to defining more precisely the notions of slow and fast.

To determine the speed (or *celerity*) of surface waves, consider an open channel with movable end wall, containing a liquid initially at rest. If the end wall is given a sudden motion, as in Fig. 11.4*a*, a wave forms and travels down the channel at some speed, c (we assume a rectangular channel of width, b, for simplicity).

If we shift coordinates so that we are traveling with the wave speed, c, we obtain a steady control volume, as shown in Fig. 11.4*b* (where for now we assume $c > \Delta V$). To obtain an expression for c, we

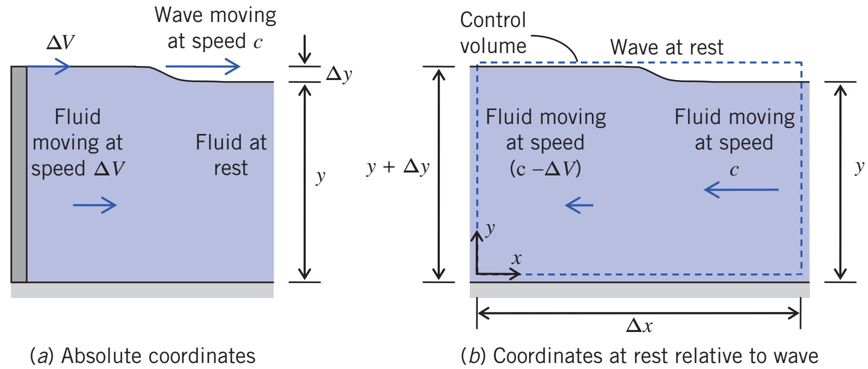

Fig. 11.4 Motion of a surface wave.

will use the continuity and momentum equations for this control volume. We also have the following assumptions:

1 Steady flow.
2 Incompressible flow.
3 Uniform velocity at each section.
4 Hydrostatic pressure distribution at each section.
5 Frictionless flow.

Assumption **1** is valid for the control volume in shifted coordinates. Assumption **2** is obviously valid for our liquid flow. Assumptions **3** and **4** are used for the entire chapter. Assumption **5** is valid in this case because we assume the area on which it acts, $b\Delta x$, is relatively small (the sketch is not to scale), so the total friction force is negligible.

For an *incompressible* flow with *uniform velocity* at each section, we can use the appropriate form of continuity from Chapter 4,

$$\sum_{CS} \vec{V} \cdot \vec{A} = 0 \tag{4.13b}$$

Applying Eq. 4.13b to the control volume, we obtain

$$(c - \Delta V)\{(y + \Delta y)b\} - cyb = 0 \tag{11.3}$$

or

$$cy - \Delta V y + c\Delta y - \Delta V \Delta y - cy = 0$$

Solving for ΔV,

$$\Delta V = c\frac{\Delta y}{y + \Delta y} \tag{11.4}$$

For the momentum equation, again with the assumption of uniform velocity at each section, we can use the following form of the x component of momentum

$$F_x = F_{S_x} + F_{B_x} = \frac{\partial}{\partial t}\int_{CV} u\rho \, d\forall + \sum_{CS} u\rho \vec{V} \cdot d\vec{A} \tag{4.18d}$$

The unsteady term $\partial/\partial t$ disappears as the flow is *steady*, and the body force F_{B_x} is zero for *horizontal flow*. So we obtain

$$F_{S_x} = \sum_{CS} u\rho \vec{V} \cdot \vec{A} \tag{11.5}$$

The surface force consists of pressure forces on the two ends, and friction force on the bottom surface (the air at the free surface contributes negligible friction in open-channel flows). By assumption **5** we neglect friction. The gage pressure at the two ends is hydrostatic, as illustrated in Fig. 11.4*b*. We recall from our study of hydrostatics that the hydrostatic force F_R on a submerged vertical surface of area A is given by the simple result

$$F_R = p_c A \tag{3.10b}$$

where p_c is the pressure at the centroid of the vertical surface. For the two vertical surfaces of the control volume, then, we have

$$\begin{aligned} F_{S_x} &= F_{R_{\text{left}}} - F_{R_{\text{right}}} = (p_c A)_{\text{left}} - (p_c A)_{\text{right}} \\ &= \left\{ \left(\rho g \frac{y+\Delta y}{2} \right)(y+\Delta y)b \right\} - \left\{ \left(\rho g \frac{y}{2} \right) yb \right\} \\ &= \frac{\rho g b}{2}(y+\Delta y)^2 - \frac{\rho g b}{2} y^2 \end{aligned}$$

Using this result in Eq. 11.5 and evaluating the terms on the right,

$$\begin{aligned} F_{S_x} &= \frac{\rho g b}{2}(y+\Delta y)^2 - \frac{\rho g b}{2} y^2 = \sum_{\text{CS}} u\rho \vec{V} \cdot \vec{A} \\ &= -(c-\Delta V)\rho\{(c-\Delta V)(y+\Delta y)b\} - c\rho\{-cyb\} \end{aligned}$$

The two terms in braces are equal, from continuity as shown in Eq. 11.3, so the momentum equation simplifies to

$$gy\Delta y + \frac{g(\Delta y)^2}{2} = yc\Delta V$$

or

$$g\left(1 + \frac{\Delta y}{2y}\right)\Delta y = c\Delta V$$

Combining this with Eq. 11.4, we obtain

$$g\left(1 + \frac{\Delta y}{2y}\right)\Delta y = c^2 \frac{\Delta y}{y+\Delta y}$$

and solving for c,

$$c^2 = gy\left(1 + \frac{\Delta y}{2y}\right)\left(1 + \frac{\Delta y}{y}\right)$$

For waves of relatively small amplitude $(\Delta y \ll y)$, we can simplify this expression to

$$c = \sqrt{gy} \tag{11.6}$$

Hence the speed of a surface disturbance depends on the local fluid depth. For example, it explains why waves "crash" as they approach the beach. Out to sea, the water depths below wave crests and troughs are approximately the same, and hence so are their speeds. As the water depth decreases on the approach to the beach, the depth of crests start to become significantly larger than trough depths, causing crests to speed up and overtake the troughs.

Note that fluid properties do not enter into the speed: Viscosity is usually a minor factor, and it turns out that the disturbance or wave we have described is due to the interaction of gravitational and inertia forces, both of which are linear with density. Equation 11.6 was derived on the basis of one-dimensional motion (x direction); a more realistic model allowing two-dimensional fluid motion (x and y directions) shows that Eq. 11.6 applies for the limiting case of large wavelength waves (Problem 11.3 explores this). Also, there are other types of surface waves, such as capillary waves driven by surface tension, for which Eq. 11.6 does not apply (Problem 11.6 explores surface tension effects). Example 11.1 illustrates the calculation for the speed of a surface wave that depends only on the depth.

The speed of surface disturbances given in Eq. 11.6 provides us with a more useful "litmus test" for categorizing the speed of a flow than the terms "slow" and "fast." To illustrate this, consider a flow

Example 11.1 SPEED OF FREE SURFACE WAVES

You are enjoying a summer's afternoon relaxing in a rowboat on a pond. You decide to find out how deep the water is by splashing your oar and timing how long it takes the wave you produce to reach the edge of the pond. (The pond is artificial; so it has approximately the same depth even to the shore.) From floats installed in the pond, you know you're 6 m from shore, and you measure the time for the wave to reach the edge to be 1.5 s. Estimate the pond depth. Does it matter if it's a freshwater pond or if it's filled with seawater?

Given: Time for a wave to reach the edge of a pond.

Find: Depth of the pond.

Solution: Use the wave speed equation, Eq. 11.6.

Governing equation: $c = \sqrt{gy}$

The time for a wave, speed c, to travel a distance L, is $\Delta t = \dfrac{L}{c}$, so $c = \dfrac{L}{\triangle t}$. Using this and Eq. 11.6,

$$\sqrt{gy} = \frac{L}{\triangle t}$$

where y is the depth, or

$$y = \frac{L^2}{g\Delta t^2}$$

Using the given data

$$y = 6^2\,\text{m}^2 \times \frac{1}{9.81}\,\frac{\text{s}^2}{\text{m}} \times \frac{1}{1.5^2\,\text{s}^2} = 1.63\text{ m} \xleftarrow{\qquad\qquad y \qquad\qquad}$$

The pond depth is about 1.63 m.

The result obtained is independent of whether the water is fresh or saline, because the speed of these surface waves is independent of fluid properties.

moving at speed V, which experiences a disturbance at some point downstream. (The disturbance could be caused by a bump in the channel floor or by a barrier, for example.) The disturbance will travel upstream at speed c *relative to the fluid*. If the fluid speed is slow, $V < c$, and the disturbance will travel upstream at absolute speed $(c - V)$. However, if the fluid speed is fast, $V > c$, and the disturbance cannot travel upstream and instead is washed downstream at absolute speed $(V - c)$. This leads to radically different responses of slow and fast flows to a downstream disturbance. Hence, recalling Eq. 11.6 for the speed c, open-channel flows may be classified on the basis of Froude number first introduced in Chapter 7:

$$Fr = \frac{V}{\sqrt{gy}} \tag{11.7}$$

Instead of the rather loose terms "slow" and "fast," we now have the following criteria:

- $\boldsymbol{Fr < 1}$ Flow is *subcritical*, *tranquil*, or *streaming*. Disturbances can travel upstream; downstream conditions can affect the flow upstream. The flow can gradually adjust to the disturbance.
- $\boldsymbol{Fr = 1}$ Flow is *critical*.
- $\boldsymbol{Fr > 1}$ Flow is *supercritical*, *rapid*, or *shooting*. No disturbance can travel upstream; downstream conditions cannot be felt upstream. The flow may "violently" respond to the disturbance because the flow has no chance to adjust to the disturbance before encountering it.

Note that for nonrectangular channels we use the hydraulic depth y_h,

$$Fr = \frac{V}{\sqrt{gy_h}} \tag{11.8}$$

These regimes of flow behavior are qualitatively analogous to the subsonic, sonic, and supersonic regimes of gas flow that we will discuss in Chapter 12. (In that case we are also comparing a flow speed, V, to the speed of a wave, c, except that the wave is a sound wave rather than a surface wave.)

We will discuss the ramifications of these various Froude number regimes later in this chapter.

11.2 *Energy Equation for Open-Channel Flows*

In analyzing open-channel flows, we will use the continuity, momentum, and energy equations. Here we derive the appropriate form of the energy equation, and continuity and momentum when needed. As in the case of pipe flow, friction in open-channel flows results in a loss of mechanical energy; this can be characterized by a head loss. The temptation is to just use one of the forms of the energy equation for pipe flow we derived in Section 8.6, such as

$$\left(\frac{p_1}{\rho g}+\alpha_1\frac{\overline{V}_2^2}{2g}+z_1\right)-\left(\frac{p_2}{\rho g}+\alpha_2\frac{\overline{V}_2^2}{2g}+z_2\right)=\frac{h_{l_T}}{g}=H_{l_T} \tag{8.30}$$

The problem with this is that it was derived on the assumption of uniform pressure at each section, which is not the case in open-channel flow (we have a hydrostatic pressure variation at each location); we do not have a uniform p_1 at section ① and uniform p_2 at section ②!

Instead we need to derive an energy equation for open-channel flows from first principles. We will closely follow the steps outlined in Section 8.6 for pipe flows but use different assumptions. You are urged to review Section 8.6 in order to be aware of the similarities and differences between pipe flows and open-channel flows.

We will use the generic control volume shown in Fig. 11.5, with the following assumptions:

1 Steady flow.
2 Incompressible flow.
3 Uniform velocity at a section.
4 Gradually varying depth so that pressure distribution is hydrostatic.
5 Small bed slope.
6 $\dot{W}_s=\dot{W}_{\text{shear}}=\dot{W}_{\text{other}}=0$.

We make a few comments here. We have seen assumptions **1–4** already; they will always apply in this chapter. Assumption **5** simplifies the analysis so that depth, y, is taken to be vertical and speed, V, is taken to be horizontal, rather than normal and parallel to the bed, respectively. Assumption **6** states that there is no shaft work, no work due to fluid shearing at the boundaries, and no other work. There is no shear work at the boundaries because on each part of the control surface the tangential velocity is zero (on the channel walls) or the shear stress is zero (the open surface), so no work can be done. Note that there can still be mechanical energy dissipation within the fluid due to friction.

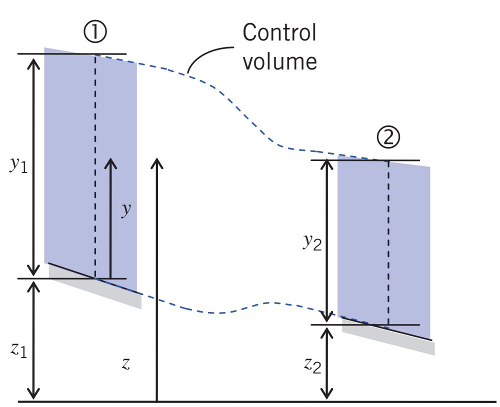

Fig. 11.5 Control volume and coordinates for energy analysis of open-channel flow.

We have chosen a generic control volume so that we can derive a generic energy equation for open-channel flows, that is, an equation that can be applied to a variety of flows such as ones with a variation in elevation, or a hydraulic jump, or a sluice gate, and so on, between sections ① and ②. Coordinate z indicates distances measured in the vertical direction; distances measured vertically from the channel bed are denoted by y. Note that y_1 and y_2 are the flow depths at sections ① and ②, respectively, and z_1 and z_2 are the corresponding channel elevations.

The energy equation for a control volume is

$$\dot{Q} - \underbrace{\cancel{\dot{W}_s}}_{=0(6)} - \underbrace{\cancel{\dot{W}_{\text{shear}}}}_{=0(6)} - \underbrace{\cancel{\dot{W}_{\text{other}}}}_{=0(6)} = \underbrace{\cancel{\frac{\partial}{\partial t}}}_{=0(1)}\int_{\text{CV}} e\rho\, d\forall + \int_{\text{CS}} (e + pv)\rho \vec{V}\cdot d\vec{A} \tag{4.56}$$

$$e = u + \frac{V^2}{2} + gz$$

Recall that u is the thermal specific energy and $v = 1/\rho$ is the specific volume. After using assumptions **1** and **6**, and rearranging, with $\dot{m} = \int \rho\vec{V}\cdot d\vec{A}$, and $dA = b\,dy$ where $b(y)$ is the channel width, we obtain

$$\begin{aligned}\dot{Q} &= -\int_1 \left(\frac{p}{\rho} + \frac{V^2}{2} + gz\right)\rho V b dy - \int_1 u\rho V b dy + \int_2 \left(\frac{p}{\rho} + \frac{V^2}{2} + gz\right)\rho V b dy + \int_2 u\rho V b dy \\ &= \int_1 \left(\frac{p}{\rho} + \frac{V^2}{2} + gz\right)\rho V b dy + \int_2 \left(\frac{p}{\rho} + \frac{V^2}{2} + gz\right)\rho V b dy + \dot{m}(u_2 - u_1)\end{aligned}$$

or

$$\int_1 \left(\frac{p}{\rho} + \frac{V^2}{2} + gz\right)\rho V b dy - \int_2 \left(\frac{p}{\rho} + \frac{V^2}{2} + gz\right)\rho V b dy = \dot{m}(u_2 - u_1) - \dot{Q} = \dot{m}h_{l_T} \tag{11.9}$$

This states that the loss in mechanical energies ("pressure," kinetic, and potential) through the control volume leads to a gain in the thermal energy and/or a loss of heat from the control volume. As in Section 8.6, these thermal effects are collected into the head loss term h_{l_T}.

The surface integrals in Eq. 11.9 can be simplified. The speed, V, is constant at each section by assumption **3**. The pressure, p, does vary across sections ① and ②, as does the potential, z. However, by assumption **4**, the pressure variation is hydrostatic. Hence, for section ①, using the notation of Fig. 11.5

$$p = \rho g(y_1 - y)$$

[so $p = \rho g y_1$ at the bed and $p = 0$ (gage) at the free surface] and

$$z = (z_1 + y)$$

Conveniently, we see that the pressure *decreases* linearly with y while z *increases* linearly with y, so the two terms together are constant,

$$\left(\frac{p}{\rho} + gz\right)_1 = g(y_1 - y) + g(z_1 + y) = g(y_1 + z_1)$$

Using these results in the first integral in Eq. 11.9,

$$\int_1 \left(\frac{p}{\rho} + \frac{V^2}{2} + gz\right)\rho V b dy = \int_1 \left(\frac{V^2}{2} + g(y_1 + z_1)\right)\rho V b dy = \left(\frac{V_1^2}{2} + gy_1 + gz_1\right)\dot{m}$$

We find a similar result for section ②, so Eq. 11.9 becomes

$$\left(\frac{V_2^2}{2} + gy_2 + gz_2\right) - \left(\frac{V_1^2}{2} + gy_1 + gz_1\right) = h_{l_T}$$

Finally, dividing by g (with $H_l = h_{l_T}/g$) leads to an energy equation for open-channel flow

$$\frac{V_1^2}{2g} + y_1 + z_1 = \frac{V_2^2}{2g} + y_2 + z_2 + H_l \tag{11.10}$$

This can be compared to the corresponding equation for pipe flow, Eq. 8.30, presented at the beginning of this section. Note that we H_l use rather than H_{l_T}; in pipe flow, we can have major and minor losses, justifying T for total, but in open-channel flow, we do not make this distinction. Equation 11.10 will prove useful to us for the remainder of the chapter and indicates that energy computations can be done simply from geometry (y and z) and velocity, V.

The *total head* or *energy head*, H, at any location in an open-channel flow can be defined from Eq. 11.10 as

$$H = \frac{V^2}{2g} + y + z \tag{11.11}$$

where y and z are the local *flow depth* and *channel bed elevation*, respectively (they no longer represent the coordinates shown in Fig. 11.5). This is a measure of the mechanical energy (kinetic and pressure/potential) of the flow. Using this in the energy equation, we obtain an alternative form

$$H_1 - H_2 = H_l \tag{11.12}$$

From this we see that the loss of total head depends on head loss due to friction.

Specific Energy

We can also define the *specific energy* (or *specific head*), denoted by the symbol E,

$$E = \frac{V^2}{2g} + y \tag{11.13}$$

This is a measure of the mechanical energy (kinetic and pressure/potential) of the flow above and beyond that due to channel bed elevation; it essentially indicates *the energy due to the flow's speed and depth*. Using Eq. 11.13 in Eq. 11.10, we obtain another form of the energy equation,

$$E_1 - E_2 + z_1 - z_2 = H_l \tag{11.14}$$

From this we see that the change in specific energy depends on friction and on channel elevation change. While the total head must decrease in the direction of flow (Eq. 11.12), the specific head may decrease, increase, or remain constant, depending on the bed elevation, z.

From continuity, $V = Q/A$, so the specific energy can be written

$$E = \frac{Q^2}{2gA^2} + y \tag{11.15}$$

For all channels, A is a monotonically increasing function of flow depth (as Table 11.1 indicates); increasing the depth must lead to a larger flow area. Hence, Eq. 11.15 indicates that the specific energy is a combination of a hyperbolic-type decrease with depth and a linear increase with depth. This is illustrated in Fig. 11.6 We see that for a given flow rate, Q, there is a range of possible flow depths and energies, but one depth at which the specific energy is at a minimum. Instead of E versus y we typically plot y versus E so that the plot corresponds to the example flow section, as shown in Fig. 11.7.

Recalling that the specific energy, E, indicates actual energy (kinetic plus potential/pressure per unit mass flow rate) being carried by the flow, we see that a given flow, Q, can have a range of energies, E, and corresponding flow depths, y. Figure 11.7 also reveals some interesting flow phenomena. For a given flow, Q, and specific energy, E, there are two possible flow depths, y; these are called *alternate depths*. For example, we can have a flow at depth y_1 or depth y_2. The first flow has large depth and is moving slowly, and the second flow is shallow but fast moving. The plot graphically indicates this: For the first flow, E_1 is made up of a large y_1 and small $V_1^2/2g$; for the second flow, E_2 is made up of a small y_2 and large $V_2^2/2g$. We will see later that we can switch from one flow to another. We can also see (as we

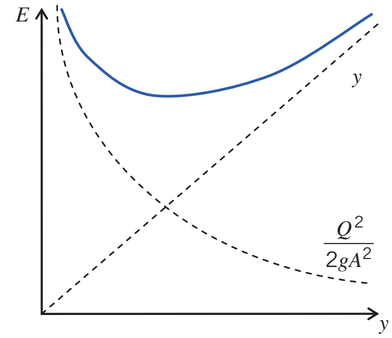

Fig. 11.6 Dependence of specific energy on flow depth for a given flow rate.

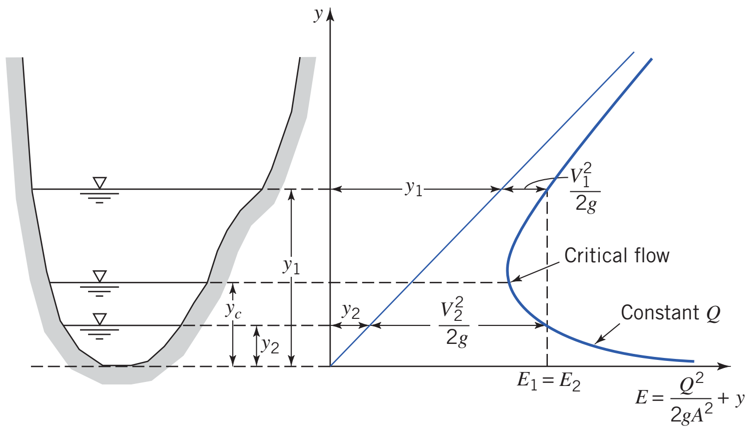

Fig. 11.7 Specific energy curve for a given flow rate.

will demonstrate in Example 11.2 for a rectangular channel) that for a given Q, there is always one flow for which the specific energy is minimum, $E = E_{min}$; we will investigate this further after Example 11.2 and show that $E_{min} = E_{crit}$, where E_{crit} is the specific energy at critical conditions.

Example 11.2 SPECIFIC ENERGY CURVES FOR A RECTANGULAR CHANNEL

For a rectangular channel of width $b = 10$ m, construct a family of specific energy curves for $Q = 0, 2, 5,$ and $10\ \text{m}^3/\text{s}$. What are the minimum specific energies for these curves?

Given: Rectangular channel and range of flow rates.

Find: Curves of specific energy. For each flow rate, find the minimum specific energy.

Solution: Use the flow rate form of the specific energy equation (Eq. 11.15) for generating the curves.

Governing equations:

$$E = \frac{Q^2}{2gA^2} + y \tag{11.15}$$

For the specific energy curves, express E as a function of depth, y.

$$E = \frac{Q^2}{2gA^2} + y = \frac{Q^2}{2g(by)^2} + y = \left(\frac{Q^2}{2gb^2}\right)\frac{1}{y^2} + y \tag{1}$$

The table and corresponding graph were generated from this equation using *Excel*.

	Specific Energy, E (m)			
y (m)	$Q = 0$	$Q = 2$	$Q = 5$	$Q = 10$
0.100	0.10	0.92	5.20	20.49
0.125	0.13	0.65	3.39	13.17
0.150	0.15	0.51	2.42	9.21
0.175	0.18	0.44	1.84	6.83
0.200	0.20	0.40	1.47	5.30
0.225	0.23	0.39	1.23	4.25
0.250	0.25	0.38	1.07	3.51
0.275	0.28	0.38	0.95	2.97
0.30	0.30	0.39	0.87	2.57
0.35	0.35	0.42	0.77	2.01
0.40	0.40	0.45	0.72	1.67
0.45	0.45	0.49	0.70	1.46
0.50	0.50	0.53	0.70	1.32
0.55	0.55	0.58	0.72	1.22
0.60	0.60	0.62	0.74	1.17
0.70	0.70	0.72	0.80	1.12
0.80	0.80	0.81	0.88	1.12
0.90	0.90	0.91	0.96	1.15
1.00	1.00	1.01	1.05	1.20
1.25	1.25	1.26	1.28	1.38
1.50	1.50	1.50	1.52	1.59
2.00	2.00	2.00	2.01	2.05
2.50	2.50	2.50	2.51	2.53

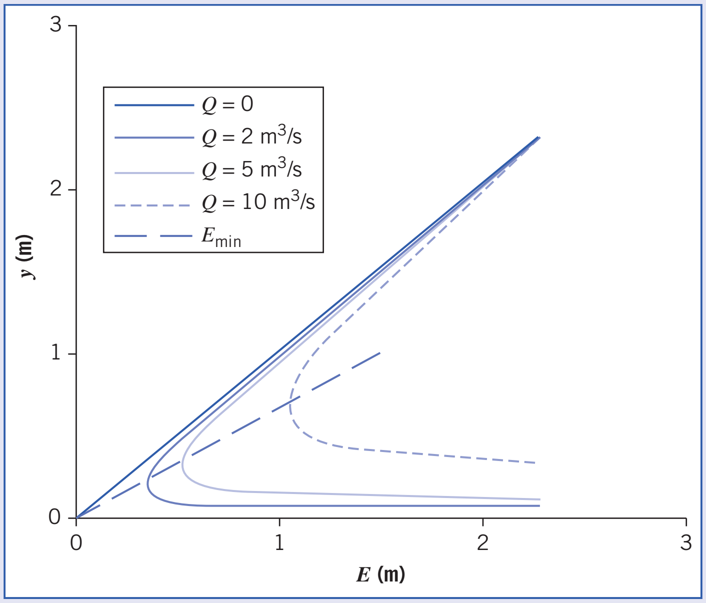

To find the minimum energy for a given Q, we differentiate Eq. 1,

$$\frac{dE}{dy} = \left(\frac{Q^2}{2gb^2}\right)\left(-\frac{2}{y^3}\right) + 1 = 0$$

Hence, the depth $y_{E_{\min}}$ for minimum specific energy is

$$y_{E_{\min}} = \left(\frac{Q^2}{gb^2}\right)^{\frac{1}{3}}$$

Using this in Eq. 11.15:

$$E_{\min} = \frac{Q^2}{2gA^2} + y_{E_{\min}} = \frac{Q^2}{2gb^2 y_{E_{\min}}^2} + \left[\frac{Q^2}{gb^2}\right]^{\frac{1}{3}} = \frac{1}{2}\left[\frac{Q^2}{gb^2}\right]\left[\frac{gb^2}{Q^2}\right]^{\frac{2}{3}} + \left[\frac{Q^2}{gb^2}\right]^{\frac{1}{3}} = \frac{3}{2}\left[\frac{Q^2}{gb^2}\right]^{\frac{1}{3}}$$

$$E_{\min} = \frac{3}{2}\left[\frac{Q^2}{gb^2}\right]^{\frac{1}{3}} = \frac{3}{2} y_{E_{\min}} \tag{2}$$

Hence for a rectangular channel, we obtain a simple result for the minimum energy. Using Eq. 2 with the given data:

Q (m^3/s)	2	5	10
$E_{\min}$ (m)	0.302	0.755	1.51

The depths corresponding to these flows are 0.201 m, 0.503 m, and 1.01 m, respectively.

We will see in the next topic that the depth at which we have minimum energy is the critical depth, y_c, and $E_{\min} = E_{crit}$.

The *Excel* workbook for this problem can be used for plotting specific energy curves for other rectangular channels. The depth for minimum energy is also obtained using *Solver*.

Critical Depth: Minimum Specific Energy

Example 11.2 treated the case of a rectangular channel. We now consider channels of general cross section. For flow in such a channel we have the specific energy in terms of flow rate Q,

$$E = \frac{Q^2}{2gA^2} + y \tag{11.15}$$

For a given flow rate Q, to find the depth for minimum specific energy, we differentiate:

$$\frac{dE}{dy} = 0 = -\frac{Q^2}{gA^3}\frac{dA}{dy} + 1 \tag{11.16}$$

To proceed further, it would seem we need $A(y)$; some examples of $A(y)$ are shown in Table 11.1. However, it turns out that for any given cross section we can write

$$dA = b_s dy \tag{11.17}$$

where, as we saw earlier, b_s is the width at the surface. This is indicated in Fig. 11.8; the incremental increase in area dA due to incremental depth change dy occurs at the free surface, where $b = b_s$.

Using Eq. 11.17 in Eq. 11.16, we find

$$-\frac{Q^2}{gA^3}\frac{dA}{dy} + 1 = -\frac{Q^2}{gA^3}b_s + 1 = 0$$

so

$$Q^2 = \frac{gA^3}{b_s} \tag{11.18}$$

for minimum specific energy. From continuity $V = Q/A$, so Eq. 11.18 leads to

$$V = \frac{Q}{A} = \frac{1}{A}\left[\frac{gA^3}{b_s}\right]^{1/2} = \sqrt{\frac{gA}{b_s}} \tag{11.19}$$

We have previously defined the hydraulic depth,

$$y_h = \frac{A}{b_s} \tag{11.2}$$

Hence, using Eq. 11.2 in Eq. 11.19, we obtain

$$V = \sqrt{gy_h} \tag{11.20}$$

But the Froude number is given by

$$Fr = \frac{V}{\sqrt{gy_h}} \tag{11.8}$$

Hence we see that, for minimum specific energy, $Fr = 1$, which corresponds to critical flow. We obtain the important result that, for flow in any open channel, *the specific energy is at its minimum at critical conditions*.

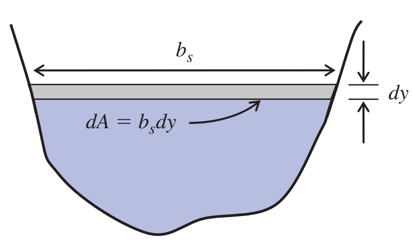

Fig. 11.8 Dependence of flow area change dA on depth change dy.

We collect Eqs. 11.18 and 11.20; for critical flow

$$Q^2 = \frac{gA_c^3}{b_{s_c}} \tag{11.21}$$

$$V_c = \sqrt{gy_{h_c}} \tag{11.22}$$

for $E = E_{\min}$. In these equations, A_c, V_c, b_{s_c}, and y_{h_c} are the critical flow area, velocity, channel surface width, and hydraulic depth, respectively. Equation 11.21 can be used to find the critical depth, y_c, for a given channel cross-sectional shape, at a given flow rate. The equation is deceptively difficult: A_c and b_{s_c} each depend on flow depth y, often in a nonlinear fashion; so it must usually be iteratively solved for y. Once y_c is obtained, area, A_c, and surface width, b_{s_c}, can be computed, leading to y_{h_c} (using Eq. 11.2). This in turn is used in Eq. 11.22 to find the flow speed V_c (or $V_c = Q/A_c$ can be used). Finally, the minimum energy can be computed from Eq. 11.15. Example 11.3 shows how the critical depth is determined for a triangular section channel.

For the particular case of a *rectangular channel*, we have $b_s = b =$ constant and $A = by$, so Eq. 11.21 becomes

$$Q^2 = \frac{gA_c^3}{b_{s_c}} = \frac{gb^3y_c^3}{b} = gb^2y_c^3$$

so

$$y_c = \left[\frac{Q^2}{gb^2}\right]^{1/3} \tag{11.23}$$

with

$$V_c = \sqrt{gy_c} = \left[\frac{gQ}{b}\right]^{1/3} \tag{11.24}$$

For the rectangular channel, a particularly simple result for the minimum energy is obtained when Eq. 11.24 is used in Eq. 11.15,

$$E = E_{min} = \frac{V_c^2}{2g} + y_c = \frac{gy_c}{2g} + y_c$$

or

$$E_{\min} = \frac{3}{2}y_c \tag{11.25}$$

This is the same result we found in Example 11.2. The critical state is an important benchmark. It will be used in the following section to help determine what happens when a flow encounters an obstacle such as a bump. Also, near the minimum E, as Fig. 11.7 shows, the rate of change of y with E is nearly infinite. This means that for critical flow conditions, even small changes in E, due to channel irregularities or disturbances, can cause pronounced changes in fluid depth. Thus, surface waves, usually in an unstable manner, form when a flow is near critical conditions. Long runs of near-critical flow consequently are avoided in practice.

Example 11.3 CRITICAL DEPTH FOR TRIANGULAR SECTION

A steep-sided triangular section channel ($\alpha = 60°$) has a flow rate of 300 m^3/s. Find the critical depth for this flow rate. Verify that the Froude number is unity.

Given: Flow in a triangular section channel.

Find: Critical depth; verify that $Fr = 1$.

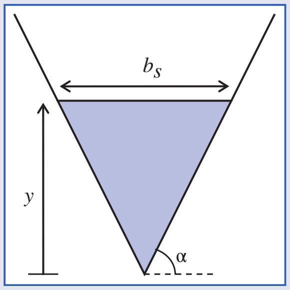

Solution: Use the critical flow equation, Eq. 11.21

Governing equations:

$$Q^2 = \frac{gA_c^3}{b_{s_c}} \qquad Fr = \frac{V}{\sqrt{gy_h}}$$

The given data is:

$$Q = 300\ \mathrm{m^3/s} \qquad \alpha = 60^\circ$$

From Table 11.1 we have the following:

$$A = y^2 \cot\alpha$$

and from basic geometry

$$\tan\alpha = \frac{y}{b_s/2} \quad \text{so} \quad b_s = 2y\cot\alpha$$

Using these in Eq. 11.21

$$Q^2 = \frac{gA_c^3}{b_{s_c}} = \frac{g[y_c^2\cot\alpha]^3}{2y_c\cot\alpha} = \frac{1}{2}gy_c^5\cot^2\alpha$$

Hence

$$y_c = \left[\frac{2Q^2\tan^2\alpha}{g}\right]^{1/5}$$

Using the given data

$$y_c = \left[2\times 300^2\left(\frac{\mathrm{m}^3}{\mathrm{s}}\right)^2 \times \tan^2\left(\frac{60\times\pi}{180}\right)\times\frac{\mathrm{s}^2}{9.81\ \mathrm{m}}\right]^{1/5} = [5.51\times 10^4\ \mathrm{m}^5]^{1/5}$$

Finally

$$y_c = 8.88\ \mathrm{m} \longleftarrow y_c$$

To verify that $Fr = 1$, we need V and y_h.
From continuity

$$V_c = \frac{Q}{A_c} = \frac{Q}{y_c^2\cot\alpha} = 300\frac{\mathrm{m}^3}{\mathrm{s}}\times\frac{1}{8.88^2\ \mathrm{m}^2}\times\frac{1}{\cot\left(\frac{60\times\pi}{180}\right)} = 6.60\ \mathrm{m/s}$$

and from the definition of hydraulic depth

$$y_{h_c} = \frac{A_c}{b_{s_c}} = \frac{y_c^2\cot\alpha}{2y_c\cot\alpha} = \frac{y_c}{2} = 4.44\ \mathrm{m}$$

Hence

$$Fr_c = \frac{V_c}{\sqrt{gy_{h_c}}} = \frac{6.60\frac{\mathrm{m}}{\mathrm{s}}}{\sqrt{9.81\frac{\mathrm{m}}{\mathrm{s}^2}\times 4.44\ \mathrm{m}}} = 1 \longleftarrow Fr_c = 1$$

We have verified that at critical depth the Froude number is unity.

As with the rectangular channel, the triangular section channel analysis leads to an explicit equation for y_c from Eq. 11.21. Other more complicated channel cross sections often lead to an implicit equation that needs to be solved numerically.

11.3 *Localized Effect of Area Change (Frictionless Flow)*

We will next consider a simple flow case in which the channel bed is horizontal and for which the effects of channel cross section (area change) predominate: flow over a bump. Since this phenomenon is localized (it takes place over a short distance), the effects of friction (on either momentum or energy) may be neglected.

The energy equation, Eq. 11.10, with the assumption of no losses due to friction then becomes

$$\frac{V_1^2}{2g}+y_1+z_1=\frac{V_2^2}{2g}+y_2+z_2=\frac{V^2}{2g}+y+z=\text{const} \tag{11.26}$$

(Note that Eq. 11.26 could have also been obtained from by applying the Bernoulli equation between two points ① and ② on the surface, because all of the requirements of the Bernoulli equation are satisfied here.) Alternatively, using the definition of specific energy

$$E_1+z_1=E_2+z_2=E+z=\text{const}$$

We see that the specific energy of a frictionless flow will change only if there is a change in the elevation of the channel bed.

Flow over a Bump

Consider frictionless flow in a horizontal rectangular channel of constant width, b, with a bump in the channel bed, as illustrated in Fig. 11.9. We choose a rectangular channel for simplicity, but the results we obtain will apply generally. The bump height above the horizontal bed of the channel is $z=h(x)$; the water depth, $y(x)$, is measured from the local channel bottom surface.

Note that we have indicated two possibilities for the free surface behavior: Perhaps the flow gradually rises over the bump; perhaps it gradually dips over the bump. One thing we can be sure of, however, is that if it rises, it will not have the same contour as the bump. (Can you explain why?) Applying the energy equation (Eq. 11.26) for frictionless flow between an upstream point ① and any point along the region of the bump,

$$\frac{V_1^2}{2g}+y_1=E_1=\frac{V^2}{2g}+y+h=E+h(x)=\text{const} \tag{11.27}$$

Equation 11.27 indicates that the specific energy must decrease through the bump, then increase back to its original value (of $E_1=E_2$),

$$E(x)=E_1-h(x) \tag{11.28}$$

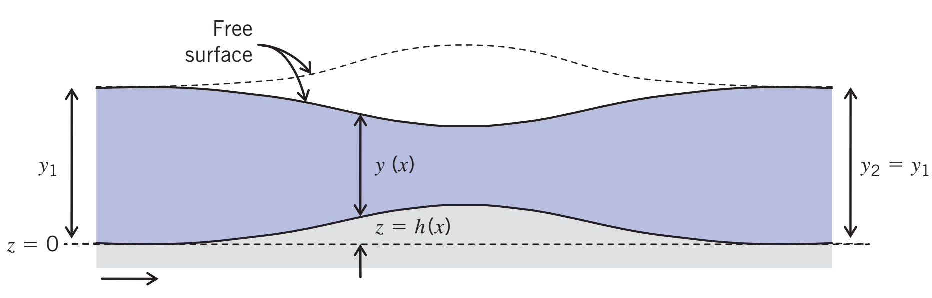

Fig. 11.9 Flow over a bump in a horizontal channel.

From continuity

$$Q = bV_1y_1 = bVy$$

Using this in Eq 11.27

$$\frac{Q^2}{2gb^2y_1^2} + y_1 = \frac{Q^2}{2gb^2y^2} + y + h = \text{const} \tag{11.29}$$

We can obtain an expression for the variation of the free surface depth by differentiating Eq. 11.29:

$$-\frac{Q^2}{gb^2y^3}\frac{dy}{dx} + \frac{dy}{dx} + \frac{dh}{dx} = 0$$

Solving for the slope of the free surface, we obtain

$$\frac{dy}{dx} = \frac{dh/dx}{\left[\frac{Q^2}{gb^2y^3} - 1\right]} = \frac{dh/dx}{\left[\frac{V^2}{gy} - 1\right]}$$

Finally,

$$\frac{dy}{dx} = \frac{1}{Fr^2 - 1}\frac{dh}{dx} \tag{11.30}$$

Equation 11.30 leads to the interesting conclusion that the response to a bump very much depends on the local Froude number, Fr.

$\boldsymbol{Fr < 1}$ Flow is *subcritical*, *tranquil*, or *streaming*. When $Fr < 1$, $(Fr^2 - 1) < 1$ and the slope dy/dx of the free surface has the *opposite* sign to the slope dh/dx of the bump: When the bump elevation increases, the flow dips; when the bump elevation decreases, the flow depth increases. This is the solid-free surface shown in Fig. 11.9.

$\boldsymbol{Fr = 1}$ Flow is *critical*. When $Fr = 1$, $(Fr^2 - 1) = 0$, Eq. 11.30 predicts an infinite water surface slope, unless dh/dx equals zero at this instant. Since the free surface slope cannot be infinite, then dh/dx must be zero when $Fr = 1$; put another way, if we have $Fr = 1$, it can *only* be at a location where $dh/dx = 0$ (at the crest of the bump, or where the channel is flat). If critical flow *is* attained, then downstream of the critical flow location the flow may be subcritical or supercritical, depending on downstream conditions. If critical flow does *not* occur where $dh/dx = 0$, then flow downstream from this location will be the same type as the flow upstream from the location.

$\boldsymbol{F_r > 1}$ Flow is *supercritical*, *rapid*, or *shooting*. When $Fr > 1$, $(Fr^2 - 1) > 1$ and the slope dy/dx of the free surface has the same sign as the slope dh/dx of the bump: when the bump elevation increases, so does the flow depth; when the bump elevation decreases, so does the flow depth. This is the dashed free surface shown in Fig. 11.9.

The general trends for $Fr < 1$ and $Fr > 1$, for either an increasing or decreasing bed elevation, are illustrated in Fig. 11.10. The important point about critical flow $(Fr = 1)$ is that, if it does occur, it can do so only where the bed elevation is constant.

An additional visual aid is provided by the specific energy graph of Fig. 11.11. This shows the specific energy curve for a given flow rate, Q. For a subcritical flow that is at state a before it encounters a bump, as the flow moves up the bump toward the bump peak, the specific energy must decrease (Eq. 11.28). Hence we move along the curve to point b. If point b corresponds to the bump peak, then we move back along the curve to a (note that this frictionless flow is reversible!) as the flow descends the bump. Alternatively, if the bump continues to increase beyond point b, we continue to move along the curve to the minimum energy point, point e where $E = E_{\text{min}} = E_{\text{crit}}$. As we have discussed, for frictionless flow to exist, point e can only be where $dh/dx = 0$ (the bump peak). For this case, something interesting happens as the flow descends down the bump: We can return along the curve to point a, or we can move along the curve to point d. This means that the surface of a subcritical flow that encounters a bump will dip and then *either* return to its original depth *or* if the bump is high enough for the flow to reach critical conditions may continue to accelerate and become shallower until it reaches the supercritical state corresponding to the original specific energy (point d). Which trend occurs depends on downstream conditions; for example, if there is some type of flow restriction, the flow downstream of the bump will return to its original subcritical state. Note that as we mentioned earlier, when a flow is at the critical

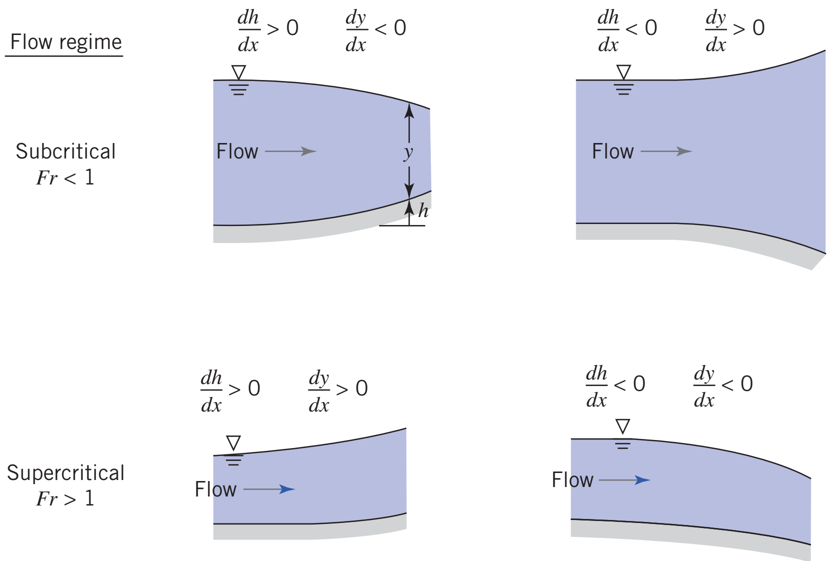

Fig. 11.10 Effects of bed elevation changes.

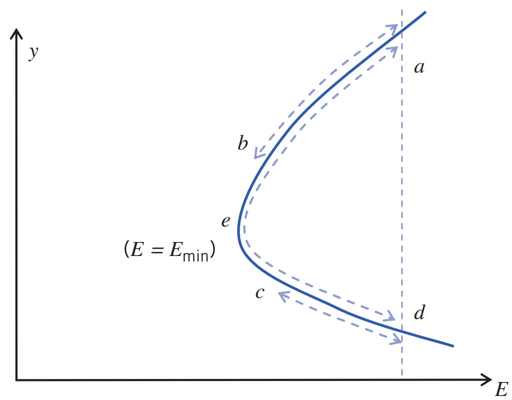

Fig. 11.11 Specific energy curve for flow over a bump.

state the surface behavior tends to display dramatic variations in behavior. Finally, Fig. 11.11 indicates that a supercritical flow (point d) that encounters a bump would increase in depth over the bump (to point c at the bump peak) and then return to its supercritical flow at point d. We also see that if the bump is high enough a supercritical flow could slow down to critical (point e) and then either return to supercritical (point d) or become subcritical (point a). Which of these possibilities actually occurs obviously depends on the bump shape, and also on upstream and downstream conditions (the last possibility is somewhat unlikely to occur in practice). In Example 11.4, the flow in a rectangular channel with a change in the bed or side wall surface is analyzed.

The alert reader may ask, "What happens if the bump is so big that the specific energy wants to decrease below the minimum shown at point e?" The answer is that the flow will no longer conform to Eq. 11.26; the flow will no longer be frictionless, because a hydraulic jump will occur, consuming a significant amount of mechanical energy (see Section 11.4).

Example 11.4 FLOW IN A RECTANGULAR CHANNEL WITH A BUMP OR A NARROWING

A rectangular channel 2 m wide has a flow of 2.4 m^3/s at a depth of 1.0 m. Determine whether critical depth occurs at (a) a section where a bump of height $h = 0.20$ m is installed across the channel bed, (b) a side wall constriction (with no bumps) reducing the channel width to 1.7 m, and (c) both the bump and side wall constrictions combined. Neglect head losses of the bump and constriction caused by friction, expansion, and contraction.

Given: Rectangular channel with a bump, a side wall constriction, or both.

Find: Whether critical flow occurs.

Solution: Compare the specific energy to the minimum specific energy for the given flow rate in each case to establish whether critical depth occurs.

Governing equations:

$$E = \frac{Q^2}{2gA^2} + y \qquad (11.15) \qquad y_c = \left[\frac{Q}{gb^2}\right]^{1/3} \qquad (11.23)$$

$$E_{min} = \frac{3}{2}y_c \qquad (11.25) \qquad E = E_1 - h \qquad (11.28)$$

(a) Bump of height $h = 0.20$ m:

The initial specific energy, E_1, is

$$E_1 = y_1 + \frac{Q^2}{2gA^2} = y_1 + \frac{Q^2}{2gb^2y_1^2}$$

$$= 1.0\text{ m} + 2.4^2\left(\frac{\text{m}^3}{\text{s}}\right)^2 \times \frac{1}{2} \times \frac{\text{s}^2}{9.81\text{ m}} \times \frac{1}{2^2\text{ m}^2} \times \frac{1}{1^2\text{ m}^2}$$

$$E_1 = 1.073\text{ m}$$

Then the specific energy at the peak of the bump, E_{bump}, is obtained from Eq. 11.28

$$E_{\text{bump}} = E_1 - h = 1.073\text{ m} - 0.20\text{ m}$$

$$E_{\text{bump}} = 0.873\text{ m} \qquad (1)$$

We must compare this to the minimum specific energy for the flow rate Q. First, the critical depth is

$$y_c = \left[\frac{Q^2}{gb^2}\right]^{1/3} = \left[2.4^2\left(\frac{\text{m}^3}{\text{s}}\right)^2 \times \frac{\text{s}^2}{9.81\text{ m}} \times \frac{1}{2^2\text{ m}^2}\right]^{1/3}$$

$$y_c = 0.528\text{ m}$$

(Note that we have $y_1 > y_c$, so we have a subcritical flow.)
Then the minimum specific energy is

$$E_{\text{min}} = \frac{3}{2}y_c = 0.791\text{ m} \qquad (2)$$

Comparing Eqs. 1 and 2 we see that with the bump we do *not* attain critical conditions.

(b) A side wall constriction (with no bump) reducing the channel width to 1.7 m:

In this case the specific energy remains constant throughout ($h = 0$), even at the constriction; so

$$E_{\text{constriction}} = E_1 - h = E_1 = 1.073\text{ m} \qquad (3)$$

However, at the constriction, we have a new value for b ($b_{\text{constriction}} = 1.7$ m), and so a new critical depth

$$y_{c_{\text{constriction}}} = \left[\frac{Q^2}{gb^2_{\text{constriction}}}\right]^{1/3} = \left[2.4^2\left(\frac{\text{m}^3}{\text{s}}\right)^2 \times \frac{\text{s}^2}{9.81\text{ m}} \times \frac{1}{1.7^2\text{ m}^2}\right]^{1/3}$$

$$y_{c_{\text{constriction}}} = 0.588\text{ m}$$

Then the minimum specific energy *at the constriction* is

$$E_{\min_{\text{constriction}}} = \frac{3}{2} y_{c_{\text{constriction}}} = 0.882 \text{ m} \tag{4}$$

Comparing Eqs. 3 and 4 we see that with the constriction we do *not* attain critical conditions.

We might enquire as to what constriction *would* cause critical flow. To find this, solve

$$E = 1.073 \text{ m} = E_{\min} = \frac{3}{2} y_c = \frac{3}{2}\left[\frac{Q^2}{gb_c^2}\right]^{1/3}$$

for the critical channel width b_c.

Hence

$$\frac{Q^2}{gb_c^2} = \left[\frac{2}{3}E_{\min}\right]^3$$

$$b_c = \frac{Q}{\sqrt{\frac{8}{27}gE_{\min}^3}}$$

$$= \left(\frac{27}{8}\right)^{1/2} \times 2.4\left(\frac{\text{m}^3}{\text{s}}\right) \times \frac{\text{s}}{9.81^{1/2}\ \text{m}^{1/2}} \times \frac{1}{1.073^{3/2}\ \text{m}^{3/2}}$$

$$b_c = 1.27 \text{ m}$$

To make the given flow attain critical conditions, the constriction should be 1.27 m; anything wider, and critical conditions are not reached.

(c) For a bump of $h = 0.20$ m *and* the constriction to $b = 1.7$ m:

We have already seen in case (a) that the bump $(h = 0.20 \text{ m})$ was insufficient by itself to create critical conditions. From case (b) we saw that at the constriction the minimum specific energy is $E_{\min} = 0.882$ m rather than $E_{\min} = 0.791$ m in the main flow. When we have both factors present, we can compare the specific energy at the bump and constriction,

$$E_{\text{bump + constriction}} = E_{\text{bump}} = E_1 - h = 0.873 \text{ m} \tag{5}$$

and the minimum specific energy for the flow at the bump and constriction,

$$E_{\min_{\text{constriction}}} = \frac{3}{2} y_{c_{\text{constriction}}} = 0.882 \text{ m} \tag{6}$$

From Eqs. 5 and 6 we see that with both factors the specific energy is actually *less* than the minimum. The fact that we must have a specific energy that is less than the minimum allowable means something has to give! What happens is that the flow assumptions become invalid; the flow may no longer be uniform or one-dimensional, or there may be a significant energy loss, for example due to a hydraulic jump occurring. (We will discuss hydraulic jumps in the following section.)

Hence the bump and constriction together *are* sufficient to make the flow reach critical state.

This problem illustrates how to determine whether a channel bump or constriction, or both, lead to critical flow conditions.

11.4 *The Hydraulic Jump*

We have shown that open-channel flow may be subcritical $(Fr < 1)$ or supercritical $(Fr > 1)$. For subcritical flow, disturbances caused by a change in bed slope or flow cross section may move upstream and downstream; the result is a smooth adjustment of the flow, as we have seen in the previous section. When flow at a section is supercritical, and downstream conditions will require a change to subcritical flow, the

(*a*) The Burdekin dam in Australia

(*b*) The Kitchen Sink (James Kilfiger)

Fig. 11.12 Examples of a hydraulic jump.

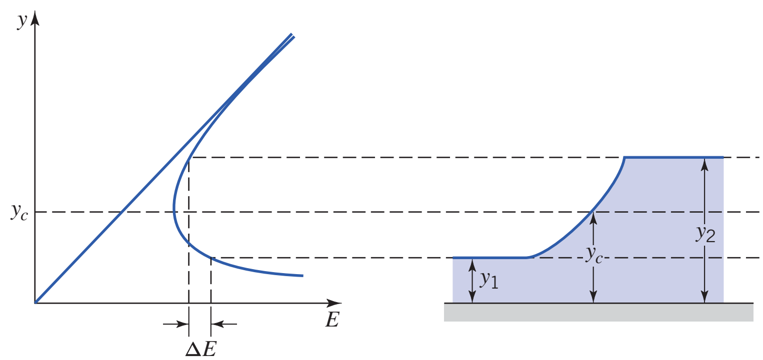

Specific energy curve

Hydraulic jump

Fig. 11.13 Specific energy curve for flow through a hydraulic jump.

need for this change cannot be communicated upstream; the flow speed exceeds the speed of surface waves, which are the mechanism for transmitting changes. Thus a gradual change with a smooth transition through the critical point is not possible. The transition from supercritical to subcritical flow occurs abruptly through a *hydraulic jump*. Hydraulic jumps can occur in canals downstream of regulating sluices, at the foot of spillways (see Fig. 11.12*a*), where a steep channel slope suddenly becomes flat—and even in the home kitchen (see Fig. 11.12*b*)! The specific energy curve and general shape of a jump are shown in Fig. 11.13. We will see in this section that the jump always goes from a supercritical depth $(y_1 < y_c)$ to a subcritical depth $(y_2 < y_c)$ and that there will be a drop ΔE in the specific energy. Unlike the changes due to phenomena such as a bump, the abrupt change in depth involves a significant loss of mechanical energy through turbulent mixing.

We shall analyze the hydraulic jump phenomenon by applying the basic equations to the control volume shown in Fig. 11.14. Experiments show that the jump occurs over a relatively short distance—

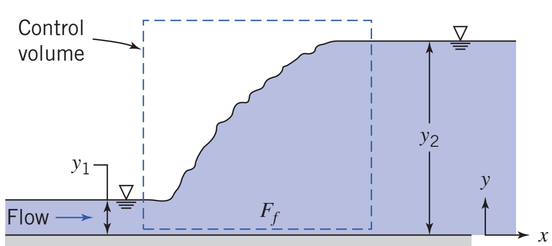

Fig. 11.14 Schematic of hydraulic jump, showing control volume used for analysis.

at most, approximately six times the larger depth (y_2) [9]. In view of this short length, it is reasonable to assume that friction force F_f acting on the control volume is negligible compared to pressure forces. Note that we are therefore ignoring viscous effects for momentum considerations, but *not* for energy considerations (as we just mentioned, there is considerable turbulence in the jump). Although hydraulic jumps can occur on inclined surfaces, for simplicity we assume a horizontal bed, and rectangular channel of width b; the results we obtain will apply generally to hydraulic jumps.

Video: A Laminar Hydraulic Jump

Hence we have the following assumptions:

1 Steady flow.
2 Incompressible flow.
3 Uniform velocity at each section.
4 Hydrostatic pressure distribution at each section.
5 Frictionless flow (for the momentum equation).

These assumptions are familiar from previous discussions in this chapter. For an *incompressible* flow with *uniform velocity* at each section, we can use the appropriate form of continuity from Chapter 4,

$$\sum_{CS} \vec{V} \cdot \vec{A} = 0 \tag{4.13b}$$

Applying Eq. 4.13b to the control volume we obtain

$$-V_1 b y_1 + V_2 b y_2 = 0$$

or

$$V_1 y_1 = V_2 y_2 \tag{11.31}$$

This is the continuity equation for the hydraulic jump. For the momentum equation, again with the assumption of uniform velocity at each section, we can use the following form for the x component of momentum

$$F_x = F_{S_x} + F_{B_x} = \frac{\partial}{\partial t}\int_{CV} u\rho \, d\forall + \sum_{CS} u\rho \vec{V} \cdot \vec{A} \tag{4.18d}$$

The unsteady term $\partial/\partial t$ disappears as the flow is *steady*, and the body force F_{B_x} is zero for *horizontal flow*. So we obtain

$$F_{S_x} = \sum_{CS} u\rho \vec{V} \cdot \vec{A} \tag{11.32}$$

The surface force consists of pressure forces on the two ends and friction force on the wetted surface. By assumption **5** we neglect friction. The gage pressure at the two ends is hydrostatic, as illustrated in Fig. 11.3*b*. We recall from our study of hydrostatics that the hydrostatic force, F_R, on a submerged vertical surface of area, A, is given by the simple result

$$F_R = p_c A \tag{3.10b}$$

where p_c is the pressure at the centroid of the vertical surface. For the two vertical surfaces of the control volume, then, we have

$$\begin{aligned} F_{S_x} &= F_{R_1} - F_{R_2} = (p_c A)_1 - (p_c A)_2 = \{(\rho g y_1) y_1 b\} - \{(\rho g y_2) y_2 b\} \\ &= \frac{\rho g b}{2}\left(y_1^2 - y_2^2\right) \end{aligned}$$

Using this result in Eq. 11.32, and evaluating the terms on the right,

$$F_{S_x} = \frac{\rho g b}{2}\left(y_1^2 - y_2^2\right) = \sum_{CS} u\rho \vec{V} \cdot \vec{A} = V_1 \rho\{-V_1 y_1 b\} + V_2 \rho\{V_2 y_2 b\}$$

Rearranging and simplifying

$$\frac{V_1^2 y_1}{g} + \frac{y_1^2}{2} = \frac{V_2^2 y_2}{g} + \frac{y_2^2}{2} \tag{11.33}$$

This is the momentum equation for the hydraulic jump. We have already derived the energy equation for open-channel flows,

$$\frac{V_1^2}{2g} + y_1 + z_1 = \frac{V_2^2}{2g} + y_2 + z_2 + H_l \tag{11.10}$$

For our horizontal hydraulic jump, $z_1 = z_2$, so

$$E_1 = \frac{V_1^2}{2g} + y_1 = \frac{V_2^2}{2g} + y_2 + H_l = E_2 + H_l \tag{11.34}$$

This is the energy equation for the hydraulic jump; the loss of mechanical energy is

$$\Delta E = E_1 - E_2 = H_l$$

The continuity, momentum, and energy equations (Eqs. 11.31, 11.33, and 11.34, respectively) constitute a complete set for analyzing a hydraulic jump.

Depth Increase Across a Hydraulic Jump

To find the downstream or, as it is called, the *sequent* depth in terms of conditions upstream from the hydraulic jump, we begin by eliminating V_2 from the momentum equation. From continuity, $V_2 = V_1 y_1/y_2$ (Eq. 11.31), so Eq. 11.33 can be written as

$$\frac{V_1^2 y_1}{g} + \frac{y_1^2}{2} = \frac{V_1^2 y_1}{g}\left(\frac{y_1}{y_2}\right) + \frac{y_2^2}{2}$$

Rearranging

$$y_2^2 - y_1^2 = \frac{2V_1^2 y_1}{g}\left(1 - \frac{y_1}{y_2}\right) = \frac{2V_1^2 y_1}{g}\left(\frac{y_2 - y_1}{y_2}\right)$$

Dividing both sides by the common factor $(y_2 - y_1)$, we obtain

$$y_2 + y_1 = \frac{2V_1^2 y_1}{g y_2}$$

Next, multiplying by y_2 and dividing by y_1^2 gives

$$\left(\frac{y_2}{y_1}\right)^2 + \left(\frac{y_2}{y_1}\right) = \frac{2V_1^2}{g y_1} = 2Fr_1^2 \tag{11.35}$$

Solving for y_2/y_1 using the quadratic formula (ignoring the physically meaningless negative root), we obtain

$$\frac{y_2}{y_1} = \frac{1}{2}\left[\sqrt{1 + 8Fr_1^2} - 1\right] \tag{11.36}$$

Hence, the ratio of downstream to upstream depths across a hydraulic jump is only a function of the upstream Froude number. Equation 11.36 has been experimentally well verified, as can be seen in Fig. 11.15*a*. Depths y_1 and y_2 are referred to as *conjugate depths*. From Eq. 11.35, we see that an increase in depth $(y_2 > y_1)$ requires an upstream Froude number greater than one $(Fr_1 > 1)$. We have not yet established that we *must* have $Fr_1 > 1$, just that it must be for an increase in depth (theoretically we could have $Fr_1 < 1$ and $y_2 < y_1$); we will now consider the head loss to demonstrate that we *must* have $Fr_1 > 1$.

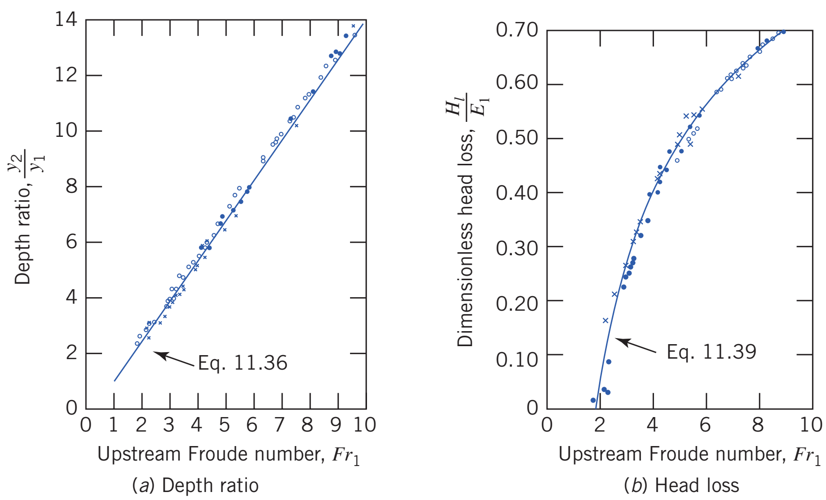

Fig. 11.15 Depth ratio and head loss for a hydraulic jump. (Data from Peterka [9].)

Head Loss Across a Hydraulic Jump

Hydraulic jumps often are used to dissipate energy below spillways as a means of preventing erosion of artificial or natural channel bottom or sides. It is therefore of interest to be able to determine the head loss due to a hydraulic jump.

From the energy equation for the jump, Eq. 11.34, we can solve for the head loss

$$H_l = E_1 - E_2 = \frac{V_1^2}{2g} + y_1 - \left(\frac{V_2^2}{2g} + y_2\right)$$

From continuity, $V_2 = V_1 y_1 / y_2$, so

$$H_l = \frac{V_1^2}{2g}\left[1 - \left(\frac{y_1}{y_2}\right)^2\right] + (y_1 - y_2)$$

or

$$\frac{H_l}{y_1} = \frac{Fr_1^2}{2}\left[1 - \left(\frac{y_1}{y_2}\right)^2\right] + \left[1 - \frac{y_2}{y_1}\right] \tag{11.37}$$

Solving Eq. 11.35 for Fr_1 in terms of y_2/y_1 and substituting into Eq.11.37, we obtain (after quite a bit of algebraic manipulation)

$$\frac{H_l}{y_1} = \frac{1}{4}\frac{\left[\frac{y_2}{y_1} - 1\right]^3}{\frac{y_2}{y_1}} \tag{11.38a}$$

Equation 11.38a is our proof that $y_2/y_1 > 1$; the left side is always positive (turbulence must lead to a loss of mechanical energy); so the cubed term must lead to a positive result. Then, from either Eq. 11.35 or Eq.11.36, we see that we must have $Fr_1 > 1$. An alternative form of this result is obtained after some minor rearranging,

$$H_l = \frac{[y_2 - y_1]^3}{4 y_1 y_2} \tag{11.38b}$$

which again shows that $y_2 > y_1$ for real flows ($H_l > 0$). Next, the specific energy, E_1, can be written as

$$E_1 = \frac{V_1^2}{2g} + y_1 = y_1\left[\frac{V_1^2}{2gy_1} + 1\right] = y_1\frac{(Fr_1^2 + 2)}{2}$$

Nondimensionalizing H_1 using E_1,

$$\frac{H_l}{E_1} = \frac{1}{2}\frac{\left[\frac{y_2}{y_1} - 1\right]^3}{\frac{y_2}{y_1}\left[Fr_1^2 + 2\right]}$$

The depth ratio in terms of Fr_1 is given by Eq. 11.36. Hence H_l/E_l can be written purely as a function of the upstream Froude number. The result, after some manipulation, is

$$\frac{H_l}{E_1} = \frac{\left[\sqrt{1+8Fr_1^2} - 3\right]^3}{8\left[\sqrt{1+8Fr_1^2} - 1\right]\left[Fr_1^2 + 2\right]} \tag{11.39}$$

We see that the head loss, as a fraction of the original specific energy across a hydraulic jump, is only a function of the upstream Froude number. Equation 11.39 is experimentally well verified, as can be seen in Fig. 11.15*b*; the figure also shows that more than 70 percent of the mechanical energy of the entering stream is dissipated in jumps with $Fr_1 > 9$. Inspection of Eq. 11.39 also shows that if $Fr_1 = 1$, then $H_l = 0$, and that negative values are predicted for $Fr_1 < 1$. Since H_l must be positive in any real flow, this reconfirms that *a hydraulic jump can occur only in supercritical flow*. *Flow downstream from a jump always is subcritical*. The characteristics of a hydraulic jump are determined in Example 11.5.

Example 11.5 HYDRAULIC JUMP IN A RECTANGULAR CHANNEL FLOW

A hydraulic jump occurs in a rectangular channel 3 m wide. The water depth before the jump is 0.6 m, and after the jump is 1.6 m. Compute (a) the flow rate in the channel (b) the critical depth (c) the head loss in the jump.

Given: Rectangular channel with hydraulic jump in which flow depth changes from 0.6 m to 1.6 m.

Find: Flow rate, critical depth, and head loss in the jump.

Solution: Use the equation that relates depths y_1 and y_2 in terms of the Froude number (Eq. 11.36); then use the Froude number (Eq. 11.7) to obtain the flow rate; use Eq. 11.23 to obtain the critical depth; and finally compute the head loss from Eq. 11.38b.

Governing equations:

$$\frac{y_2}{y_1} = \frac{1}{2}\left[-1 + \sqrt{1+8Fr_1^2}\right] \tag{11.36}$$

$$Fr = \frac{V}{\sqrt{gy}} \tag{11.7}$$

$$y_c = \left[\frac{Q^2}{gb^2}\right]^{1/3} \tag{11.23}$$

$$H_l = \frac{[y_2 - y_1]^3}{4y_1y_2} \tag{11.38b}$$

(a) From Eq. 11.36

$$Fr_1 = \sqrt{\frac{\left(1 + 2\frac{y_2}{y_1}\right)^2 - 1}{8}}$$

$$= \sqrt{\frac{\left(1 + 2\times\frac{1.6\text{ m}}{0.6\text{ m}}\right)^2 - 1}{8}}$$

$$Fr_1 = 2.21$$

As expected, $Fr_1 > 1$ (supercritical flow). We can now use the definition of Froude number for open-channel flow to find V_1

$$Fr_1 = \frac{V_1}{\sqrt{gy_1}}$$

Hence

$$V_1 = Fr_1\sqrt{gy_1} = 2.21 \times \sqrt{\frac{9.81\ \text{m}}{\text{s}^2} \times 0.6\ \text{m}} = 5.36\ \text{m/s}$$

From this we can obtain the flow rate, Q.

$$Q = by_1V_1 = 3.0\ \text{m} \times 0.6\ \text{m} \times \frac{5.36\ \text{m}}{\text{s}}$$

$$Q = 9.65\ \text{m}^3/\text{s} \longleftarrow Q$$

(b) The critical depth can be obtained from Eq. 11.23.

$$y_c = \left[\frac{Q^2}{gb^2}\right]^{1/3} = \left(9.65^2\frac{\text{m}^6}{\text{s}^2} \times \frac{\text{s}^2}{9.81\ \text{m}} \times \frac{1}{3.0^2\ \text{m}^2}\right)^{1/3}$$

$$y_c = 1.02\ \text{m} \longleftarrow y_c$$

Note that as illustrated in Fig. 11.13, $y_1 < y_c < y_2$.

(c) The head loss can be found from Eq. 11.38b.

$$H_l = \frac{[y_2 - y_1]^3}{4y_1y_2} = \frac{1}{4}\frac{[1.6\ \text{m} - 0.6\ \text{m}]^3}{1.6\ \text{m} \times 0.6\ \text{m}} = 0.260\ \text{m} \longleftarrow H_l$$

As a verification of this result, we use the energy equation directly,

$$H_l = E_1 - E_2 = \left(y_1 + \frac{V_1^2}{2g}\right) - \left(y_2 + \frac{V_2^2}{2g}\right)$$

with $V_2 = Q/(by_2) = 2.01\ \text{m/s}$,

$$H_l = \left(0.6\ \text{m} + 5.36^2\frac{\text{m}^2}{\text{s}^2} \times \frac{1}{2} \times \frac{\text{s}^2}{9.81\ \text{m}}\right) - \left(1.6\ \text{m} + 2.01^2\frac{\text{m}^2}{\text{s}^2} \times \frac{1}{2} \times \frac{\text{s}^2}{9.81\ \text{m}}\right)$$

$$H_l = 0.258\ \text{m}$$

This problem illustrates computation of flow rate, critical depth, and head loss, for a hydraulic jump.

11.5 *Steady Uniform Flow*

After studying local effects such as bumps and hydraulic jumps, and defining some fundamental quantities such as the specific energy and critical velocity, we are ready to analyze flows in long stretches. Steady uniform flow is something that is to be expected to occur for channels of constant slope and cross section; Figs. 11.1 and 11.2 show examples of this kind of flow. Such flows are very common and important and have been extensively studied.

The simplest such flow is *fully developed* flow; it is analogous to fully developed flow in pipes. A fully developed flow is one for which the channel is *prismatic*, that is, a channel with constant slope and cross section that flows at constant depth. This depth, y_n, is termed the *normal depth* and the flow is

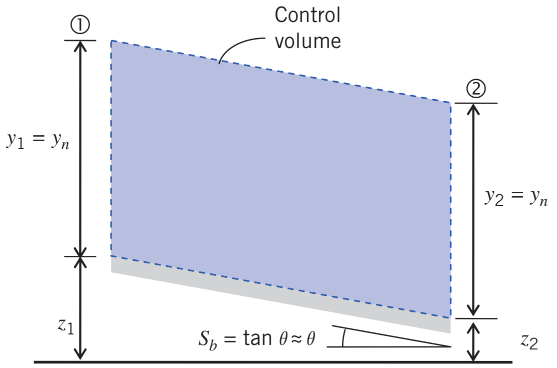

Fig. 11.16 Control volume for uniform channel flow.

termed a *uniform flow*. Hence the expression *uniform flow* in this chapter has a different meaning than in earlier chapters. In earlier chapters it meant that the *velocity* was uniform *at a section* of the flow; in this chapter we use it to mean that, but in addition specifically that the *flow* is the same *at all sections*. Hence for the flow shown in Fig. 11.16, we have $A_1 = A_2 = A$ (cross-sectional areas), $Q_1 = Q_2 = Q$ (flow rates), $V_1 = V_2 = V$ (average velocity, $V = Q/A$), and $y_1 = y_2 = y_n$ (flow depth).

As before (Section 11.2), we use the following assumptions:

1 Steady flow.
2 Incompressible flow.
3 Uniform velocity at a section.
4 Gradually varying depth so that pressure distribution is hydrostatic.
5 Bed slope is small.
6 $\dot{W}_s = \dot{W}_{\text{shear}} = \dot{W}_{\text{other}} = 0.$

Note that assumption **5** means that we can approximate the flow depth y to be vertical and flow speed horizontal. (Strictly speaking they should be normal and parallel to the channel bottom, respectively.)

The continuity equation is obvious for this case.

$$Q = V_1 A_1 = V_2 A_2 = VA$$

For the momentum equation, again with the assumption of uniform velocity at each section, we can use the following form for the x component of momentum

$$F_x = F_{S_x} + F_{B_x} = \frac{\partial}{\partial t}\int_{\text{CV}} u\rho\, d\forall + \sum\nolimits_{\text{CS}} u\rho\, \vec{V}\cdot\vec{A} \tag{4.18d}$$

The unsteady term $\partial/\partial t$ disappears as the flow is steady, and the control surface summation is zero because $V_1 = V_2$; hence the right-hand side is zero as there is no change of momentum for the control volume. The body force $F_{B_x} = W \sin\theta$ where W is the weight of fluid in the control volume; θ is the bed slope, as shown in Fig. 11.16. The surface force consists of the hydrostatic force on the two end surfaces at ① and ② and the friction force F_f on the wetted surface of the control volume; however, because we have the same pressure distributions at ① and ②, the net x component of pressure force is zero. Using all these results in Eq. 4.18d we obtain

$$-F_f + W\sin\theta = 0$$

or

$$F_f = W\sin\theta \tag{11.40}$$

We see that for flow at normal depth, the component of the gravity force driving the flow is just balanced by the friction force acting on the channel walls. This is in contrast to flow in a pipe or duct, for which (with the exception of pure gravity driven flow) we usually have a balance between an applied pressure gradient and the friction. The friction force may be expressed as the product of an average wall shear stress, τ_w, and the channel wetted surface area, PL (where L is the channel length), on which the stress acts

$$F_f = \tau_w PL \tag{11.41}$$

The component of gravity force can be written as

$$W \sin\theta = \rho g A L \sin\theta \approx \rho g A L \theta \approx \rho g A L S_b \tag{11.42}$$

where S_b is the channel bed slope. Using Eqs. 11.41 and 11.42 in Eq. 11.40,

$$\tau_w PL = \rho g A L S_b$$

or

$$\tau_w = \frac{\rho g A S_b}{P} = \rho g R_h S_b \tag{11.43}$$

where we have used the hydraulic radius, $R_h = A/P$ as defined in Eq. 11.1. In Chapter 9, we have previously introduced a skin friction coefficient,

$$C_f = \frac{\tau_w}{\frac{1}{2}\rho V^2} \tag{9.22}$$

Using this in Eq. 11.43

$$\frac{1}{2} C_f \rho V^2 = \rho g R_h S_b$$

so, solving for V

$$V = \sqrt{\frac{2g}{C_f}}\sqrt{R_h S_b} \tag{11.44}$$

The Manning Equation for Uniform Flow

Equation 11.44 gives the flow velocity V as a function of channel geometry, specifically the hydraulic radius, R_h and slope, S_b, but also the skin friction coefficient, C_f. This latter term is difficult to obtain experimentally or theoretically; it depends on a number of factors such as bed roughness and fluid properties, but also on the velocity itself (via the flow Reynolds number). Instead of this we define a new quantity,

$$C = \sqrt{\frac{2g}{C_f}}$$

so that Eq. 11.44 becomes

$$V = C\sqrt{R_h S_b} \tag{11.45}$$

Equation 11.45 is the well-known *Chezy equation*, and C is referred to as the *Chezy coefficient*. Experimental values of C were obtained by Manning [10]. He suggested that

$$C = \frac{1}{n} R_h^{1/6} \tag{11.46}$$

where n is a roughness coefficient having different values for different types of boundary roughness. Some representative values of n are listed in Table 11.2. The range of values given in the table reflects the importance of surface characteristics. For the same material, the value of n can vary 20 to 30 percent depending on the finish of the channel surface. Substituting C from Eq. 11.46 into Eq. 11.45 results in the *Manning equation* for the velocity for flow at normal depth

$$V = \frac{1}{n} R_h^{2/3} S_b^{1/2} \tag{11.47a}$$

Table 11.2
Representative Manning's Roughness Coefficients

Channel Type	Condition	Manning's n
Constructed, unlined	Smooth earth	0.016 – 0.020
	Bare earth	0.018 – 0.022
	Gravel	0.022 – 0.030
	Rocky	0.025 – 0.035
Constructed, lined	Plastic	0.009 – 0.011
	Asphalt	0.013 – 0.016
	Concrete	0.013 – 0.015
	Brick	0.014 – 0.017
	Wood	0.011 – 0.015
	Masonry	0.025 – 0.030
	Corrugated metal	0.022 – 0.024
Natural	Stream, clean	0.025 – 0.035
	Major river, clean	0.030 – 0.040
	Major river, sluggish	0.040 – 0.080

Source: Data taken from References [1], [3], [7], [11], [12]

which is valid for SI units. Manning's equation in SI units can also be expressed as

$$Q = \frac{1}{n} A R_h^{2/3} S_b^{1/2}$$

where A is in square feet. Note that a number of these equations, as well as many that follow, are "engineering" equations; that is, *the user needs to be aware of the required units of each term in the equation*.

The relationship among variables in Eqs. can be viewed in a number of ways. For example, it shows that the volume flow rate through a prismatic channel of given slope and roughness is a function of both channel size and channel shape. This is illustrated in Examples 11.6 and 11.7.

Example 11.6 FLOW RATE IN A RECTANGULAR CHANNEL

An 2.4 m wide rectangular channel with a bed slope of 0.0004 m/m has a depth of flow of 0.6 m. Assuming steady uniform flow, determine the discharge in the channel. The Manning roughness coefficient is $n = 0.015$.

Given: Geometry of rectangular channel and flow depth.

Find: Flow rate Q.

Solution: Use the appropriate form of Manning's equation.

Governing equations:

$$Q = \frac{1}{n} A R_h^{2/3} S_b^{1/2} \qquad R_h = \frac{by}{b + 2y} \qquad \text{(Table 11.1)}$$

Using this equation with the given data

$$Q = \frac{1}{n} A R_h^{2/3} S_b^{1/2}$$

$$= \left[\frac{1}{0.015} \times (2.4\,\text{m} \times 0.6\,\text{m}) \left(\frac{2.4\,\text{m} \times 0.6\,\text{m}}{2.4\,\text{m} + 2 \times 0.6\,\text{m}} \right)^{2/3} \times \left(0.0004 \frac{\text{m}}{\text{m}} \right)^{1/2} \right]$$

$$Q = 1.04\,\text{m}^3/\text{s} \xleftarrow{\qquad\qquad\qquad\qquad Q \qquad\qquad\qquad\qquad}$$

This problem demonstrates use of Manning's equation to solve for flow rate, Q. Note that because this is an "engineering" equation, the units do not cancel.

Example 11.7 FLOW VERSUS AREA THROUGH TWO CHANNEL SHAPES

Open channels, of square and semicircular shapes, are being considered for carrying flow on a slope of $S_b = 0.001$; the channel walls are to be poured concrete with $n = 0.015$. Evaluate the flow rate delivered by the channels for maximum dimensions between 0.5 and 2.0 m. Compare the channels on the basis of volume flow rate for given cross-sectional area.

Given: Square and semicircular channels; $S_b = 0.001$ and $n = 0.015$. Sizes between 0.5 and 2.0 m across.

Find: Flow rate as a function of size. Compare channels on the basis of volume flow rate, Q, versus cross-sectional area, A.

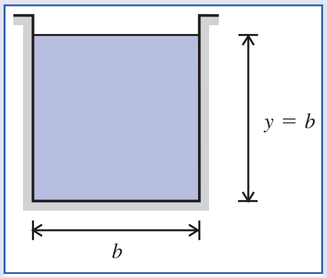

Solution: Use the appropriate form of Manning's equation.

Governing equations:

$$Q = \frac{1}{n} A R_h^{2/3} S_b^{1/2}$$

Assumption: Flow at normal depth.

For the square channel,

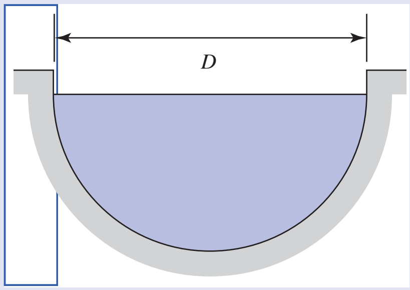

$$P = 3b \quad \text{and} \quad A = b^2 \quad \text{so} \quad R_h = \frac{b}{3}$$

Using this in Equation

$$Q = \frac{1}{n} A R_h^{2/3} S_b^{1/2} = \frac{1}{n} b^2 \left(\frac{b}{3} \right)^{2/3} S_b^{1/2} = \frac{1}{3^{2/3} n} S_b^{1/2} b^{8/3}$$

For $b = 1$ m,

$$Q = \frac{1}{3^{2/3}(0.015)} (0.001)^{1/2} (1)^{8/3} = 1.01\,\text{m}^3/\text{s} \xleftarrow{\qquad\qquad\qquad Q \qquad\qquad\qquad}$$

Tabulating for a range of sizes yields

b (m)	0.5	1.0	1.5	2.0
A (m^2)	0.25	1.00	2.25	4.00
Q (m^3/s)	0.160	1.01	2.99	6.44

For the semicircular channel,

$$P = \frac{\pi D}{2} \quad \text{and} \quad A = \frac{\pi D^2}{8}$$

$$\text{so} \quad R_h = \frac{\pi D^2}{8}\,\frac{2}{\pi D} = \frac{D}{4}$$

Using this in Equation

$$Q = \frac{1}{n} A R_h^{2/3} S_b^{1/2} = \frac{1}{n}\frac{\pi D^2}{8}\left(\frac{D}{4}\right)^{2/3} S_b^{1/2}$$

$$= \frac{\pi}{4^{5/3}(2)n} S_b^{1/2} D^{8/3}$$

For $D = 1$ m,

$$Q = \frac{\pi}{4^{5/3}(2)(0.015)}(0.001)^{1/2}(1)^{8/3} = 0.329\ \text{m}^3/\text{s} \longleftarrow Q$$

Tabulating for a range of sizes yields

D (m)	0.5	1.0	1.5	2.0
A (m^2)	0.0982	0.393	0.884	1.57
Q (m^3/s)	0.0517	0.329	0.969	2.09

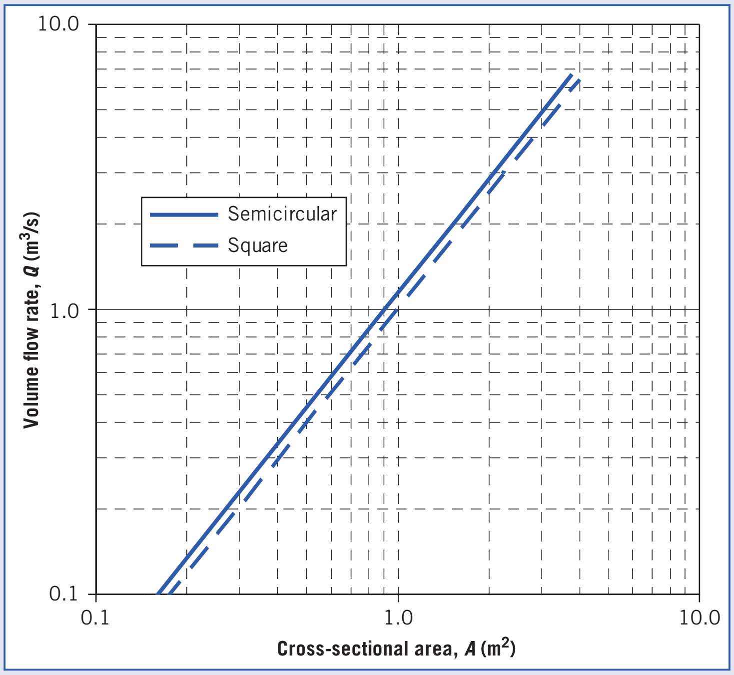

For both channels, volume flow rate varies as

$$Q \sim L^{8/3} \quad \text{or} \quad Q \sim A^{4/3}$$

since $A \sim L^2$. The plot of flow rate versus cross-sectional area shows that the semicircular channel is more "efficient."

Performance of the two channels may be compared at any specified area. At $A = 1\ \text{m}^2$, $Q/A = 1.01$ m/s for the square channel. For the semicircular channel with $A = 1\ \text{m}^2$, then $D = 1.60$ m, and $Q = 1.15\ \text{m}^3/\text{s}$; so $Q/A = 1.15$ m/s. Thus the semicircular channel carries approximately 14 percent more flow per unit area than the square channel.

The comparison on cross-sectional area is important in determining the amount of excavation required to build the channel. The channel shapes also could be compared on the basis of perimeter, which would indicate the amount of concrete needed to finish the channel.

The *Excel* workbook for this problem can be used for computing data and plotting curves for other square and semicircular channels.

We have demonstrated that Eq. 11.48 means that, for normal flow, the flow rate depends on the channel size and shape. For a specified flow rate through a prismatic channel of given slope and roughness, Eq. 11.48 also shows that the depth of uniform flow is a function of both channel size and shape, as well as the slope. There is only one depth for uniform flow at a given flow rate; it may be greater than, less than, or equal to the critical depth. This is illustrated in Examples 11.8 and 11.9.

Example 11.8 NORMAL DEPTH IN A RECTANGULAR CHANNEL

Determine the normal depth (for uniform flow) if the channel described in Example 11.6 has a flow rate of 100 cfs.

Given: Geometric data on rectangular channel of Example 11.6.

Find: Normal depth for a flow rate $Q = 2.83\ \text{m}^3/\text{s}$.

Solution: Use the appropriate form of Manning's equation. For a problem in English Engineering units, this is Eq. 11.48b.

Governing equations:

$$Q = \frac{1.49}{n} A R_h^{2/3} S_b^{1/2} \qquad R_h = \frac{b y_n}{b + 2y_n} \quad \text{Table}(11.1)$$

Combining these equations

$$Q = \frac{1.49}{n} A R_h^{2/3} S_b^{1/2} = \frac{1.49}{n}(b y_n)\left(\frac{b y_n}{b + 2y_n}\right)^{2/3} S_b^{1/2}$$

Hence, after rearranging

$$\left(\frac{Qn}{1.49 b^{5/3} S_b^{1/2}}\right)^3 (b + 2y_n)^2 = y_n^5$$

Substituting $Q = 2.83\ \text{m}^3/\text{s}$, $n = 0.015$, $b = 2.4$ m, and $S_b = 0.0004$ and simplifying (remembering this is an "engineering" equation, in which we insert values without units),

$$0.48(8 + 2y_n)^2 = y_n^5$$

This nonlinear equation can be solved for y_n using a numerical method such as the Newton–Raphson method (or better yet using your calculator's solving feature or *Excel*'s *Goal Seek* or *Solver*!). We find

$$y_n = 1.232\ \text{m} \xleftarrow{\qquad\qquad y_n \qquad\qquad}$$

Note that there are five roots, but four of them are complex—mathematically correct but physically meaningless.

- This problem demonstrates the use of Manning's equation for finding the normal depth.
- This relatively simple physical problem still involved solving a nonlinear algebraic equation.

The *Excel* workbook for this problem can be used for solving similar problems.

Example 11.9 DETERMINATION OF FLUME SIZE

An above-ground flume, built from timber, is to convey water from a mountain lake to a small hydroelectric plant. The flume is to deliver water at $Q = 2\ \text{m}^3/\text{s}$; the slope is $S_b = 0.002$ and $n = 0.013$. Evaluate the required flume size for (a) a rectangular section with $y/b = 0.5$ and (b) an equilateral triangular section.

Given: Flume to be built from timber, with $S_b = 0.002$, $n = 0.013$, and $Q = 2.00\ \text{m}^3/\text{s}$.

Find: Required flume size for:
(a) Rectangular section with $y/b = 0.5$.
(b) Equilateral triangular section.

Solution: Assume flume is long, so flow is uniform; it is at normal depth. Then Eq. 11.48a applies.

Governing equations:

$$Q = \frac{1}{n} A R_h^{2/3} S_b^{1/2} \tag{11.48a}$$

The choice of channel shape fixes the relationship between R_h and A; so Eq. 11.48a may be solved for normal depth, y_n, thus determining the channel size required.

(a) Rectangular section

$$P = 2y_n + b;\ y_n/b = 0.5 \text{ so } b = 2y_n$$
$$P = 2y_n + 2y_n = 4y_n \qquad A = y_n b = y_n(2y_n) = 2y_n^2$$
$$\text{so } R_h = \frac{A}{P} = \frac{2y_n^2}{4y_n} = 0.5y_n$$

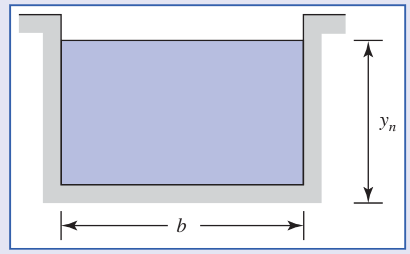

Using this in Eq. 11.48a,

$$Q = \frac{1}{n} A R_h^{2/3} S_b^{1/2} = \frac{1}{n}(2y_n^2)(0.5y_n)^{2/3} S_b^{1/2} = \frac{2(0.5)^{2/3}}{n} y_n^{8/3} S_b^{1/2}$$

Solving for y_n

$$y_n = \left[\frac{nQ}{2(0.5)^{2/3} S_b^{1/2}}\right]^{3/8} = \left[\frac{0.013(2.00)}{2(0.5)^{2/3}(0.002)^{1/2}}\right]^{3/8} = 0.748 \text{ m}$$

The required dimensions for the rectangular channel are

$$y_n = 0.748 \text{ m} \quad A = 1.12 \text{ m}^2$$
$$b = 1.50 \text{ m} \quad p = 3.00 \text{ m}$$

Flume size

(b) Equilateral triangle section

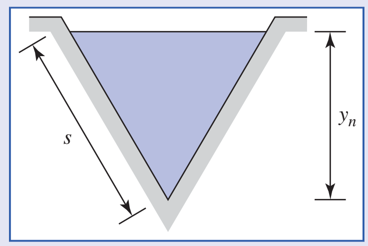

$$P = 2s = \frac{2y_n}{\cos 30°} \qquad A = \frac{y_n s}{2} = \frac{y_n^2}{2 \cos 30°}$$

$$\text{so } R_h = \frac{A}{P} = \frac{y_n}{4}$$

Using this in Eq. 11.48a,

$$Q = \frac{1}{n} A R_h^{2/3} S_b^{1/2} = \frac{1}{n}\left(\frac{y_n^2}{2 \cos 30°}\right)\left(\frac{y_n}{4}\right)^{2/3} S_b^{1/2} = \frac{1}{2 \cos 30° (4)^{2/3} n} y_n^{8/3} S_b^{1/2}$$

Solving for y_n

$$y_n = \left[\frac{2 \cos 30° (4)^{2/3} nQ}{S_b^{1/2}}\right]^{3/8} = \left[\frac{2 \cos 30° (4)^{2/3}(0.013)(2.00)}{(0.002)^{1/2}}\right]^{3/8} = 1.42 \text{ m}$$

The required dimensions for the triangular channel are

$$y_n = 1.42 \text{ m} \qquad A = 1.16 \text{ m}^2$$
$$b_s = 1.64 \text{ m} \qquad p = 3.28 \text{ m}$$

Flume size

Note that for the triangular channel

$$V = \frac{Q}{A} = 2.0 \frac{\text{m}^3}{\text{s}} \times \frac{1}{1.16 \text{ m}^2} = 1.72 \text{ m/s}$$

and

$$Fr = \frac{V}{\sqrt{g y_h}} = \frac{V}{\sqrt{gA/b_s}}$$

$$Fr = 1.72 \frac{\text{m}}{\text{s}} \times \frac{1}{\left[9.81 \frac{\text{m}}{\text{s}^2} \times 1.16 \text{ m}^2 \times \frac{1}{1.64 \text{ m}}\right]^{1/2}} = 0.653$$

Hence this normal flow is subcritical (as is the flow in the rectangular channel).

Comparing results, we see that the rectangular flume would be cheaper to build; its perimeter is about 8.5 percent less than that of the triangular flume.

This problem shows the effect of channel shape on the size required to deliver a given flow at a specified bed slope and roughness coefficient. At specified S_b and n, flow may be subcritical, critical, or supercritical, depending on Q.

Energy Equation for Uniform Flow

To complete our discussion of normal flows, we consider the energy equation. The energy equation was already derived in Section 11.2.

$$\frac{V_1^2}{2g} + y_1 + z_1 = \frac{V_2^2}{2g} + y_2 + z_2 + H_l \tag{11.10}$$

In this case we obtain, with $V_1 = V_2 = V$, and $y_1 = y_2 = y_n$,

$$z_1 = z_2 + H_l$$

or

$$H_l = z_1 - z_2 = LS_b \tag{11.49}$$

where S_b is the slope of the bed and L is the distance between points ① and ②. Hence we see that for flow at normal depth, *the head loss due to friction is equal to the change in elevation of the bed*. The specific energy, E, is the same at all sections,

$$E = E_1 = \frac{V_1^2}{2g} + y_1 = E_2 = \frac{V_2^2}{2g} + y = \text{const}$$

For completeness we also compute the energy grade line EGL and hydraulic grade line HGL. From Section 6.4

$$EGL = \frac{p}{\rho g} + \frac{V^2}{2g} + z_{\text{total}} \tag{6.16b}$$

and

$$HGL = \frac{p}{\rho g} + z_{\text{total}} \tag{6.16c}$$

Note that we have used $z_{\text{total}} = z + y$ in Eqs. 6.16b and 6.16c (in Chapter 6, z is the total elevation of the free surface). Hence at any point on the free surface (recall that we are using gage pressures),

$$EGL = \frac{V^2}{2g} + z + y \tag{11.50}$$

and

$$HGL = z + y \tag{11.51}$$

Hence, using Eqs. 11.50 and 11.51 in Eq. 11.10, between points ① and ②, we obtain

$$EGL_1 - EGL_2 = H_l = z_1 - z_2$$

and (because $V_1 = V_2$)

$$HGL_1 - HGL_2 = H_l = z_1 - z_2$$

For normal flow, the energy grade line, the hydraulic grade line, and the channel bed are all parallel. The trends for the energy grade line, hydraulic grade line, and specific energy are shown in Fig. 11.17.

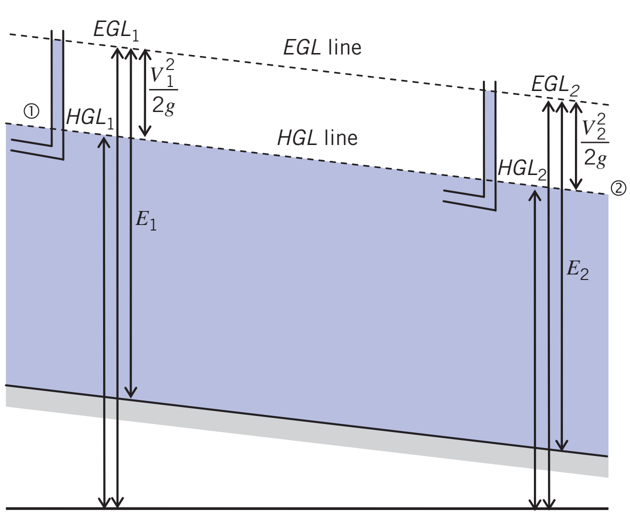

Fig. 11.17 Energy grade line, hydraulic grade line, and specific energy for uniform flow.

Optimum Channel Cross Section

For given slope and roughness, the optimum channel cross section is that for which we need the smallest channel for a given flow rate; this is when Q/A is maximized. From Eq. 11.48a (using the SI version, although the results we obtain will apply generally)

$$\frac{Q}{A} = \frac{1}{n} R_h^{2/3} S_b^{1/2} \tag{11.52}$$

Thus the optimum cross section has maximum hydraulic radius, R_h. Since $R_h = A/P$, R_h is maximum when the wetted perimeter is minimum. Solving Eq. 11.52 for A (with $R_h = A/P$) then yields

$$A = \left[\frac{nQ}{S_b^{1/2}}\right]^{3/5} P^{2/5} \tag{11.53}$$

From Eq. 11.53, the flow area will be a minimum when the wetted perimeter is a minimum.

Wetted perimeter, P, is a function of channel shape. For any given prismatic channel shape (rectangular, trapezoidal, triangular, circular, etc.), the channel cross section can be optimized. Optimum cross sections for common channel shapes are given without proof in Table 11.3.

Once the optimum cross section for a given channel shape has been determined, expressions for normal depth, y_n, and area, A, as functions of flow rate can be obtained from Eq. 11.48a. These expressions are included in Table 11.3.

Table 11.3
Properties of Optimum Open-Channel Sections (SI Units)

Shape	Section	Optimum Geometry	Normal Depth, y_n	Cross-Sectional Area, A
Trapezoidal	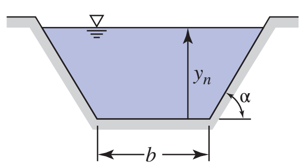	$\alpha = 60°$ $b = \frac{2}{\sqrt{3}} y_n$	$0.968\left[\frac{Qn}{S_b^{1/2}}\right]^{3/8}$	$1.622\left[\frac{Qn}{S_b^{1/2}}\right]^{3/4}$
Rectangular	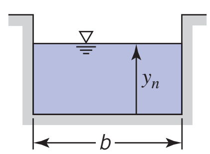	$b = 2y_n$	$0.917\left[\frac{Qn}{S_b^{1/2}}\right]^{3/8}$	$1.682\left[\frac{Qn}{S_b^{1/2}}\right]^{3/4}$
Triangular	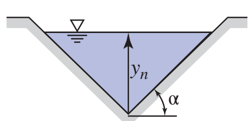	$\alpha = 45°$	$1.297\left[\frac{Qn}{S_b^{1/2}}\right]^{3/8}$	$1.682\left[\frac{Qn}{S_b^{1/2}}\right]^{3/4}$
Wide Flat	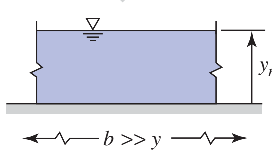	None	$1.00\left[\frac{(Q/b)n}{S_b^{1/2}}\right]^{3/8}$	—
Circular	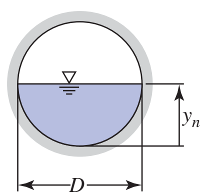	$D = 2y_n$	$1.00\left[\frac{Qn}{S_b^{1/2}}\right]^{3/8}$	$1.583\left[\frac{Qn}{S_b^{1/2}}\right]^{3/4}$

11.6 *Flow with Gradually Varying Depth*

Most human-made channels are designed to have uniform flow (for example, see Fig. 11.1). However, this is not true in some situations. A channel can have nonuniform flow, that is, a flow for which the depth and hence speed, and so on vary along the channel for a number of reasons. Examples include when an open-channel flow encounters a change in bed slope, geometry, or roughness, or is adjusting itself back to normal depth after experiencing an upstream change (such as a sluice gate). We have already studied rapid, localized changes, such as that occurring in a hydraulic jump, but here we assume flow depth changes gradually. Flow with gradually varying depth is analyzed by applying the energy equation to a differential control volume; the result is a differential equation that relates changes in depth to distance along the flow. The resulting equation may be solved analytically or, more typically numerically, if *we approximate the head loss at each section as being the same as that for flow at normal depth, using the velocity and hydraulic radius of the section*. Water depth and channel bed height are assumed to change slowly. As in the case of flow at normal depth, velocity is assumed uniform, and the pressure distribution is assumed hydrostatic at each section.

The energy equation (Eq. 11.10) for open-channel flow was applied to a finite control volume in Section 11.2,

$$\frac{V_1^2}{2g} + y_1 + z_1 = \frac{V_2^2}{2g} + y_2 + z_2 + H_l \tag{11.10}$$

We apply this equation to the differential control volume, of length dx, shown in Fig. 11.18. Note that *the energy grade line, hydraulic grade line, and channel bottom all have different slopes*, unlike for the uniform flow of the previous section!

The energy equation becomes

$$\frac{V^2}{2g} + y + z = \frac{V^2}{2g} + d\left(\frac{V^2}{2g}\right) + y + dy + z + dz + dH_l$$

or after simplifying and rearranging

$$-d\left(\frac{V^2}{2g}\right) - dy - dz = dH_l \tag{11.54}$$

This is not surprising. The differential loss of mechanical energy equals the differential head loss. From channel geometry

$$dz = -S_b dx \tag{11.55}$$

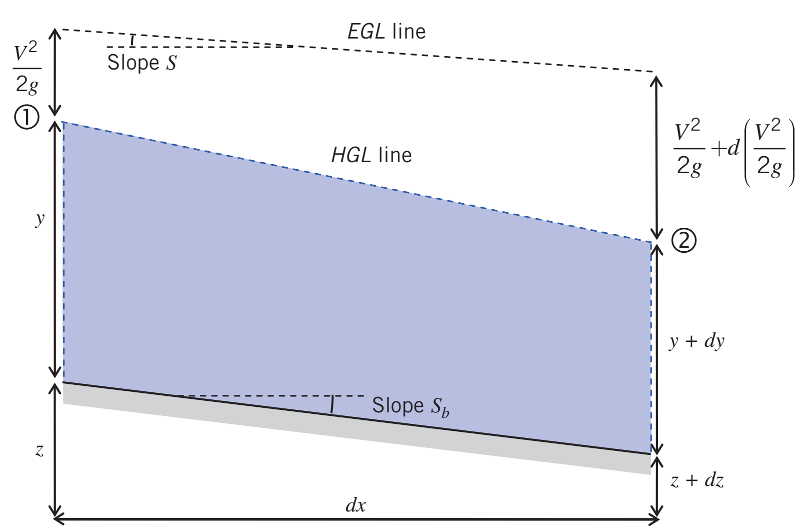

Fig. 11.18 Control volume for energy analysis of gradually varying flow.

We also have the approximation that the head loss in this differential nonuniform flow can be approximated by the head loss that uniform flow would have at the same flow rate, Q, at the section. Hence the differential head loss is approximated by

$$dH_l = S dx \tag{11.56}$$

where S is the slope of the EGL (see Fig. 11.18). Using Eqs. 11.55 and 11.56 in Eq. 11.54, dividing by dx, and rearranging, we obtain

$$\frac{d}{dx}\left(\frac{V^2}{2g}\right) + \frac{dy}{dx} = S_b - S \tag{11.57}$$

To eliminate the velocity derivative, we differentiate the continuity equation, $Q = VA = \text{const}$, to obtain

$$\frac{dQ}{dx} = 0 = A\frac{dV}{dx} + V\frac{dA}{dx}$$

or

$$\frac{dV}{dx} = -\frac{V}{A}\frac{dA}{dx} = -\frac{Vb_s}{A}\frac{dy}{dx} \tag{11.58}$$

where we have used $dA = b_s dy$ (Eq. 11.17), where b_s is the channel width at the free surface. Using Eq. 11.58 in Eq. 11.57, after rearranging

$$\frac{d}{dx}\left(\frac{V^2}{2g}\right) + \frac{dy}{dx} = \frac{V}{g}\frac{dV}{dx} + \frac{dy}{dx} = -\frac{V^2 b_s}{gA}\frac{dy}{dx} + \frac{dy}{dx} = S_b - S \tag{11.59}$$

Next, we recognize that

$$\frac{V^2 b_s}{gA} = \frac{V^2}{g\dfrac{A}{b_s}} = \frac{V^2}{g y_h} = Fr^2$$

where y_h is the hydraulic depth (Eq. 11.2). Using this in Eq. 11.59, we finally obtain our desired form of the *energy equation for gradually varying flow*

$$\frac{dy}{dx} = \frac{S_b - S}{1 - Fr^2} \tag{11.60}$$

This equation indicates how the depth y of the flow varies. Whether the flow becomes deeper ($dy/dx > 0$) or shallower ($dy/dx < 0$) depends on the sign of the right-hand side. For example, consider a channel that has a horizontal section ($S_b = 0$):

$$\frac{dy}{dx} = -\frac{S}{1 - Fr^2}$$

Because of friction the EGL always decreases, so $S > 0$. If the incoming flow is subcritical ($Fr < 1$), the flow depth will gradually decrease ($dy/dx < 0$); if the incoming flow is supercritical ($Fr > 1$), the flow depth will gradually increase ($dy/dx > 0$). Note also that for critical flow ($Fr = 1$), the equation leads to a singularity, and gradually flow is no longer sustainable—something dramatic will happen (guess what).

Calculation of Surface Profiles

Equation 11.60 can be used to solve for the free surface shape $y(x)$; the equation looks simple enough, but it is usually difficult to solve analytically and so is solved numerically. It is difficult to solve because the bed slope, S_b, the local Froude number, Fr, and S, the EGL slope equivalent to uniform flow at rate Q, will in general all vary with location, x. For S, we use the results obtained in Section 11.5, specifically

$$Q = \frac{1}{n} A R_h^{2/3} S^{1/2}$$

Note that we have used S rather than S_b in Eq. 11.48 as we are using the equation to obtain an *equivalent* value of S for a uniform flow at rate Q! Solving for S,

$$S = \frac{n^2 Q^2}{A^2 R_h^{4/3}} \tag{11.61a}$$

We can also express the Froude number as a function of Q,

$$Fr = \frac{V}{\sqrt{g y_h}} = \frac{Q}{A\sqrt{g y_h}} \tag{11.62}$$

Using Eq. 11.61a (or) and 11.62 in Eq. 11.60

$$\frac{dy}{dx} = \frac{S_b - S}{1 - Fr^2} = \frac{S_b - \dfrac{n^2 Q^2}{A^2 R_h^{4/3}}}{1 - \dfrac{Q^2}{A^2 g y_h}} \tag{11.63a}$$

For a given channel (slope, S_b, and roughness coefficient, n, both of which may vary with x) and flow rate Q, the area A, hydraulic radius R_h, and hydraulic depth y_h are all functions of depth y (see Section 11.1). Hence Eq. 11.63 are usually best solved using a suitable numerical integration scheme. Example 11.10 shows such a calculation for the simplest case, that of a rectangular channel.

Example 11.10 CALCULATION OF FREE SURFACE PROFILE

Water flows in a 5-m-wide rectangular channel made from unfinished concrete with $n = 0.015$. The channel contains a long reach on which S_b is constant at $S_b = 0.020$. At one section, flow is at depth $y_1 = 1.5$ m, with speed $V_1 = 4.0$ m/s. Calculate and plot the free surface profile for the first 100 m of the channel and find the final depth.

Given: Water flow in a rectangular channel.

Find: Plot of free surface profile; depth at 100 m.

Solution: Use the appropriate form of the equation for flow depth, Eq. 11.63a.

Governing equations:

$$\frac{dy}{dx} = \frac{S_b - S}{1 - Fr^2} = \frac{S_b - \dfrac{n^2 Q^2}{A^2 R_h^{4/3}}}{1 - \dfrac{Q^2}{A^2 g y_h}} \tag{11.63a}$$

We use Euler's method (see Section 5.5) to convert the differential equation to a difference equation. In this approach, the differential is converted to a difference,

$$\frac{dy}{dx} \approx \frac{\Delta y}{\Delta x} \tag{1}$$

where Δx and Δy are small but finite changes in x and y, respectively. Combining Eqs. 11.63a and 1, and rearranging,

$$\Delta y = \Delta x \left(\frac{S_b - \dfrac{n^2 Q^2}{A^2 R_h^{4/3}}}{1 - \dfrac{Q^2}{A^2 g y_h}} \right)$$

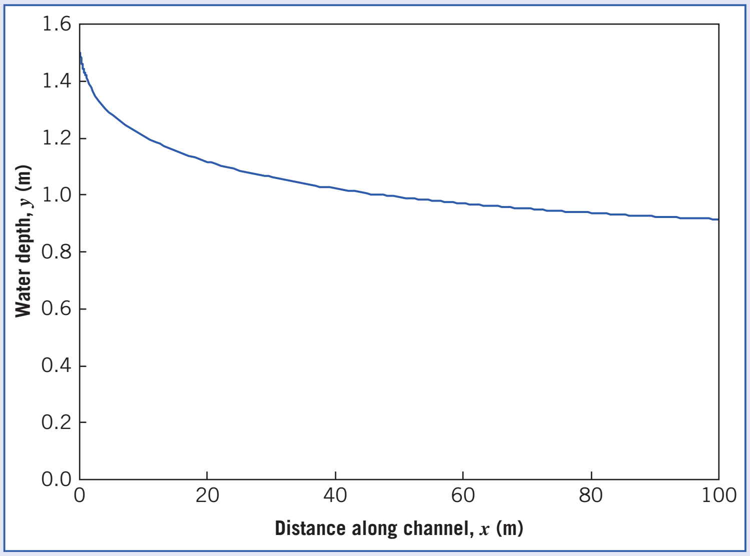

Finally, we let $\Delta y = y_{i+1} - y_i$, where y_i and y_{i+1} are the depths at point i and a point $(i+1)$ distance Δx further downstream,

$$y_{i+1} = y_i + \Delta x \left(\frac{S_{b_i} - \dfrac{n_i^2 Q^2}{A_i^2 R_{h_i}^{4/3}}}{1 - \dfrac{Q^2}{A_i^2 g y_{h_i}}} \right) \tag{2}$$

Equation 2 computes the depth, y_{i+1}, given data at point i. In the current application, S_b and n are constant, but A, R_h, and y_h will, of course, vary with x because they are functions of y. For a rectangular channel we have the following:

$$A_i = b y_i$$

$$R_{h_i} = \frac{b y_i}{b + 2 y_i}$$

$$y_{h_i} = \frac{A_i}{b_s} = \frac{A_i}{b} = \frac{b y_i}{b_s} = y_i$$

The calculations are conveniently performed and results plotted using *Excel*. Note that partial results are shown in the table and that for the first meter, over which there is a rapid change in depth, the step size is $\Delta x = 0.05$.

i	x (m)	y (m)	A (m^2)	R_h (m)	y_h (m)
1	0.00	1.500	7.500	0.938	1.500
2	0.05	1.491	7.454	0.934	1.491
3	0.10	1.483	7.417	0.931	1.483
4	0.15	1.477	7.385	0.928	1.477
5	0.20	1.471	7.356	0.926	1.471
⋮	⋮	⋮	⋮	⋮	⋮
118	98	0.916	4.580	0.670	0.916
119	99	0.915	4.576	0.670	0.915
120	100	0.914	4.571	0.669	0.914

The depth at location $x = 100$ m is seen to be 0.914 m.

$y(100\ \text{m}) = 0.914\ \text{m}$ ← $y(100\ \text{m})$

Note (following the solution procedure of Example 11.8) that the normal depth for this flow is $y_n = 0.858$ m; the flow depth is asymptotically approaching this value. In general, this is one of several possibilities, depending on the values of the initial depth and the channel properties (slope and roughness). A flow may approach normal depth, become deeper and deeper, or eventually become shallower and experience a hydraulic jump.

The accuracy of the results obtained obviously depends on the numerical model used; for example, a more accurate model is the RK4 method. Also, for the first meter or so, there are rapid changes in depth, bringing into question the validity of several assumptions, for example, uniform flow and hydrostatic pressure.

The *Excel* workbook for this problem can be modified for use in solving similar problems.

11.7 *Discharge Measurement Using Weirs*

A *weir* is a device (or overflow structure) that is placed normal to the direction of flow. The weir essentially backs up water so that, in flowing over the weir, the water goes through critical depth. Weirs have been used for the measurement of water flow in open channels for many years. Weirs can generally be classified as *sharp-crested weirs* and *broad-crested weirs*. Weirs are discussed in detail in Bos [13], Brater [14], and Replogle [15].

A *sharp-crested weir* is basically a thin plate mounted perpendicular to the flow with the top of the plate having a beveled, sharp edge, which makes the nappe spring clear from the plate (see Fig. 11.19).

The rate of flow is determined by measuring the head, typically in a stilling well (see Fig. 11.20) at a distance upstream from the crest. The head H is measured using a gage.

Suppressed Rectangular Weir

These sharp-crested weirs are as wide as the channel and the width of the nappe is the same length as the crest. Referring to Fig. 11.20, consider an elemental area $dA = bdh$ and assume the velocity is $V = \sqrt{2gh}$; then the elemental flow is

$$dQ = bdh\sqrt{2gh} = b\sqrt{2g}h^{1/2}dh$$

The discharge is expressed by integrating this over the area above the top of the weir crest:

$$Q = \int_0^H dQ = \sqrt{2g}b\int_0^H h^{1/2}dh = \frac{2}{3}\sqrt{2g}bH^{3/2} \tag{11.64}$$

Friction effects have been neglected in the derivation of Eq. 11.64. The drawdown effect shown in Fig. 11.19 and the crest contraction indicate that the streamlines are not parallel or normal to the area in the plane. To account for these effects, a coefficient of discharge C_d is used, so that

$$Q = C_d\frac{2}{3}\sqrt{2g}bH^{3/2}$$

where C_d is approximately 0.62. This is the basic equation for a suppressed rectangular weir, which can be expressed more generally as

$$Q = C_w bH^{3/2} \tag{11.65}$$

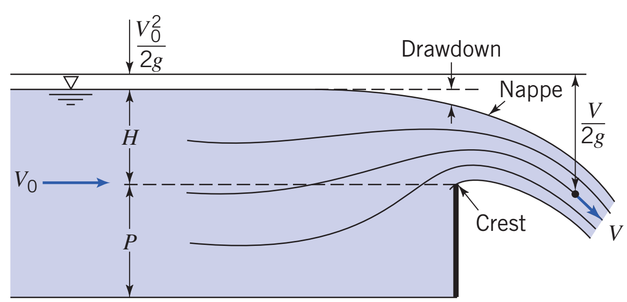

Fig. 11.19 Flow over sharp-crested weir.

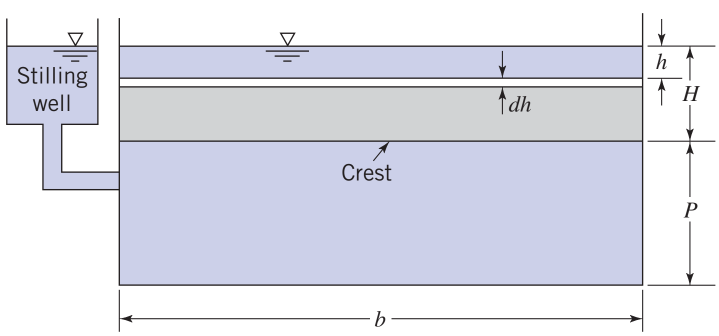

Fig. 11.20 Rectangular sharp-crested weir without end contraction.

where the C_w is the weir coefficient, $C_w = \frac{2}{3}C_d\sqrt{2g}$, and for SI units, $C_w \approx 1.84$.

If the velocity of approach, V_a, where H is measured is appreciable, then the integration limits are

$$Q = \sqrt{2g}b \int_{V_a^2/2g}^{H+V_a^2/2g} h^{1/2}dh = C_w b\left[\left(H + \frac{V_a^2}{2g}\right)^{3/2} - \left(\frac{V_a^2}{2g}\right)^{3/2}\right] \tag{11.66}$$

When $(V_a^2/2g)^{3/2} \approx 0$ Eq. 11.66 can be simplified to

$$Q = C_w b\left(H + \frac{V_a^2}{2g}\right)^{3/2} \tag{11.67}$$

Contracted Rectangular Weirs

A *contracted horizontal weir* is another sharp-crested weir with a crest that is shorter than the width of the channel and one or two beveled end sections so that water contracts both horizontally and vertically. This forces the nappe width to be less than b. The effective crest length is

$$b' = b - 0.1\,nH$$

where $n = 1$ if the weir is placed against one side wall of the channel so that the contraction on one side is suppressed and $n = 2$ if the weir is positioned so that it is not placed against a side wall.

Triangular Weir

Triangular or *V-notch weirs* are sharp-crested weirs that are used for relatively small flows but that have the advantage that they can also function for reasonably large flows as well. Referring to Fig. 11.21, the rate of discharge through an elemental area, dA, is

$$dQ = C_d\sqrt{2gh}dA$$

where $dA = 2xdh$, and $x = (H-h)\tan(\theta/2)$; so $dA = 2(H-h)\tan(\theta/2)dh$. Then

$$dQ = C_d\sqrt{2gh}\left[2(H-h)\tan\left(\frac{\theta}{2}\right)dh\right]$$

and

$$Q = C_d 2\sqrt{2g}\tan\left(\frac{\theta}{2}\right)\int_0^H (H-h)h^{1/2}dh$$

$$= C_d\left(\frac{8}{15}\right)\sqrt{2g}\tan\left(\frac{\theta}{2}\right)H^{5/2}$$

$$Q = C_w H^{5/2}$$

The value of C_w for a value of $\theta = 90°$; (the most common) is $C_w = 1.38$ for SI units.

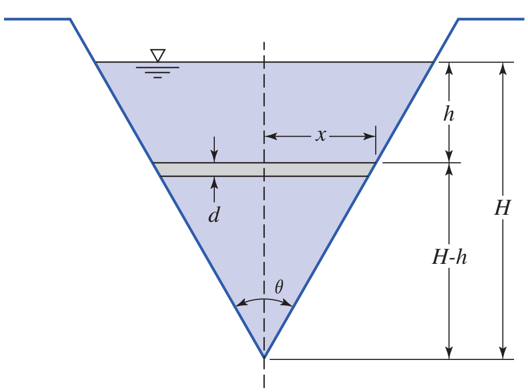

Fig. 11.21 Triangular sharp-crested weir.

Broad-Crested Weir

Broad-crested weirs (Fig. 11.22) are essentially critical-depth weirs in that if the weirs are high enough, critical depth occurs on the crest of the weir. For critical flow conditions $y_c = (Q^2/gb^2)^{1/3}$ (Eq. 11.23) and $E = 3y_c/2$ (Eq. 11.25) for rectangular channels:

$$Q = b\sqrt{gy_c^3} = b\sqrt{g\left(\frac{2}{3}E\right)^3} = b\left(\frac{2}{3}\right)^{3/2}\sqrt{g}E^{3/2}$$

or, assuming the approach velocity is negligible:

$$Q = b\left(\frac{2}{3}\right)^{3/2}\sqrt{g}H^{3/2}$$
$$Q = C_w bH^{3/2}$$

Figure 11.23 illustrates a broad-crested weir installation in a trapezoidal canal.

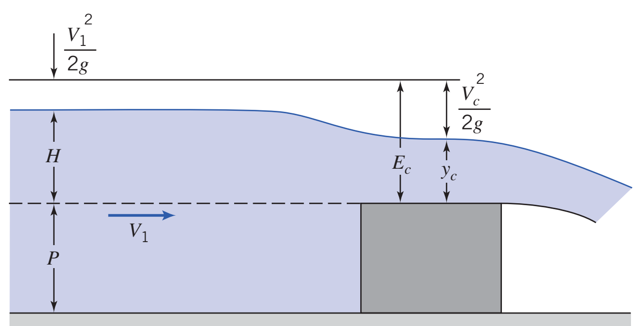

Fig. 11.22 Broad-crested weir.

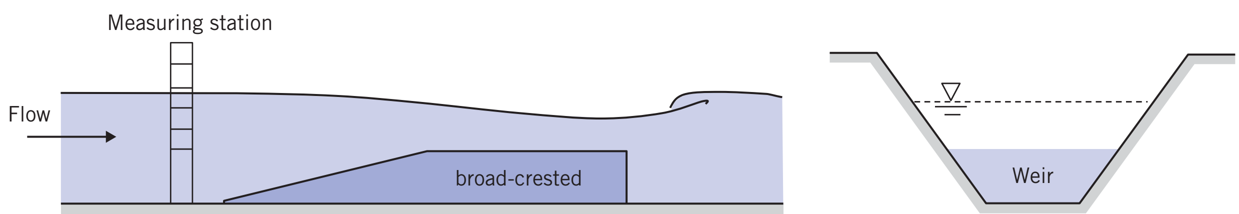

Fig. 11.23 Broad-crested weir in trapezoidal canal.

Example 11.11 shows the process for calculating the flow over a sharp-crested weir. The procedure for other weir geometries is basically the same as for this specific geometry.

Example 11.11 DISCHARGE FROM A RECTANGULAR SHARP-CRESTED SUPPRESSED WEIR

A rectangular, sharp-crested suppressed weir 3 m long is 1 m high. Determine the discharge when the head is 150 mm.

Given: Geometry and head of a rectangular sharp-crested suppressed weir.

Find: Discharge (flow rate), Q.

Solution: Use the appropriate weir discharge equation.

Governing equation:

$$Q = C_w bH^{3/2} \tag{11.65}$$

In Eq. 11.65 we use $C_w \approx 1.84$, and the given data, $b = 3$ m and $H = 150\text{ mm} = 0.15$ m, so

$$Q = 1.84 \times 3\text{ m} \times (0.15\text{ m})^{3/2}$$
$$Q = 0.321\text{ m}^3/\text{s}$$

Q

Note that Eq. 11.65 is an "engineering" equation; so we do not expect the units to cancel.

This problem illustrates use of one of a number of weir discharge equations.

11.8 *Summary and Useful Equations*

In this chapter, we:

✓ Derived an expression for the speed of surface waves and developed the notion of the specific energy of a flow and derived the Froude number for determining whether a flow is subcritical, critical, or supercritical.
✓ Investigated rapidly varied flows, especially the hydraulic jump.
✓ Investigated steady uniform flow in a channel and used energy and momentum concepts to derive Chezy's and Manning's equations.
✓ Investigated some basic concepts of gradually varied flows.

We also learned how to use many of the important concepts mentioned above in analyzing a range of real-world open-channel flow problems.

Note: Most of the equations in the table below have a number of constraints or limitations—*be sure to refer to their page numbers for details*!

Useful Equations

Hydraulic radius:	$R_h = \dfrac{A}{P}$	(11.1)	Page 510
Hydraulic depth:	$y_h = \dfrac{A}{b_s}$	(11.2)	Page 510
Speed of surface wave:	$c = \sqrt{gy}$	(11.6)	Page 513
Froude number:	$Fr = \dfrac{V}{\sqrt{gy}}$	(11.7)	Page 514
Energy equation for open-channel flow:	$\dfrac{V_1^2}{2g} + y_1 + z_1 = \dfrac{V_2^2}{2g} + y_2 + z_2 + H_l$	(11.10)	Page 516
Total head:	$H = \dfrac{V^2}{2g} + y + z$	(11.11)	Page 517
Specific energy:	$E = \dfrac{V^2}{2g} + y$	(11.13)	Page 517
Critical flow:	$Q^2 = \dfrac{gA_c^3}{b_{s_c}}$	(11.21)	Page 521
Critical velocity:	$V_c = \sqrt{gy_{h_c}}$	(11.22)	Page 521
Critical depth (rectangular channel):	$y_c = \left[\dfrac{Q^2}{gb^2}\right]^{1/3}$	(11.23)	Page 521
Critical velocity (rectangular channel):	$V_c = \sqrt{gy_c} = \left[\dfrac{gQ}{b}\right]^{1/3}$	(11.24)	Page 521
Minimum specific energy (rectangular channel):	$E_{\min} = \dfrac{3}{2}y_c$	(11.25)	Page 521
Hydraulic jump conjugate depths:	$\dfrac{y_2}{y_1} = \dfrac{1}{2}\left[\sqrt{1+8Fr_1^2}-1\right]$	(11.36)	Page 530

Table (*Continued*)

Hydraulic jump head loss:	$H_l = \dfrac{[y_2 - y_1]^3}{4y_1y_2}$	(11.38b)	Page 531
Hydraulic jump head loss (in terms of Fr_1):	$\dfrac{H_l}{E_1} = \dfrac{\left[\sqrt{1+8Fr_1^2}-3\right]^3}{8\left[\sqrt{1+8Fr_1^2}-1\right][Fr_1^2+2]}$	(11.39)	Page 532
Chezy equation:	$V = C\sqrt{R_hS_b}$	(11.45)	Page 535
Chezy coefficient:	$C = \dfrac{1}{n}R_h^{1/6}$	(11.46)	Page 535
Manning equation for velocity (SI units)	$V = \dfrac{1}{n}R_h^{2/3}S_b^{1/2}$	(11.47a)	Page 535
Manning equation for flow (SI units)	$Q = \dfrac{1}{n}AR_h^{2/3}S_b^{1/2}$		Page 536
Energy Grade Line	$EGL = \dfrac{V^2}{2g} + z + y$	(11.50)	Page 541
Hydraulic Grade Line	$HGL = z + y$	(11.51)	Page 541
Energy equation (gradually varying flow):	$\dfrac{dy}{dx} = \dfrac{S_b - S}{1 - Fr^2}$	(11.60)	Page 544

REFERENCES

1. Chow, V. T., *Open-Channel Hydraulics*. New York: McGraw-Hill, 1959.

2. Henderson, F. M., *Open-Channel Flow*. New York: Macmillan, 1966.

3. "Manning's Roughness Coefficient," The Engineer's Toolbox, http://www.engineeringtoolbox.com/mannings-roughness-d_799.html (accessed September 22, 2014).

4. Townson, J. M., *Free-Surface Hydraulics*. London: Unwin Hyman, 1991.

5. Chaudhry, M. H., *Open-Channel Flow*. Englewood Cliffs, NJ: Prentice Hall, 1993.

6. Jain, S. C., *Open Channel Flow*. New York: Wiley, 2001.

7. "Design Charts for Open Channel Flow," HDS 3, Federal Highway Association, 1961, http://www.fhwa.dot.gov/engineering/hydraulics/pubs/hds3.pdf.

8. Mays, L. W., *Water Resources Engineering*, 2005 ed. New York: Wiley, 2005.

9. Peterka, A. J., "Hydraulic Design of Stilling Basins and Energy Dissipators," U.S. Department of the Interior, Bureau of Reclamation, Engineering Monograph No. 25 (Revised), July 1963.

10. Manning, R., " On the Flow of Water in Open Channels and Pipes." *Transactions Institute of Civil Engineers of Ireland*, vol. *20*, pp. 161–209, Dublin, 1891; Supplement, vol. 24, pp. 179–207, 1895.

11. Linsley, R. K., J. B. Franzini, D. L. Freyberg, and G. Tchobanoglous, *Water Resources Engineering*. New York: McGraw-Hill, 1991.

12. Chen, Y. H., and G. K. Cotton, *Design of Roadside Channels with Flexible Linings*, Hydraulic Engineering Circular 15, FHWA-IP-87-7, Federal Highway Administration, McClean, VA, 1988.

13. Bos, M. G., J. A. Replogle, and A. J. Clemmens, *Flow Measuring Flumes for Open Channel System*. New York: John Wiley & Sons, 1984.

14. Brater, E. F., H. W. King, J. E. Lindell, and C. Y. Wei, *Handbook of Hydraulics*, 7th ed. New York: McGraw-Hill, 1996.

15. Replogle, J. A., A. J. Clemmens, and C. A. Pugh, "Hydraulic Design of Flow Measuring Structures." *Hydraulic Design Handbook*, L. W. Mays, ed. New York: McGraw-Hill, 1999.

PROBLEMS

Basic Concepts and Definitions

11.1 Verify the equation given in Table 11.1 for the hydraulic radius of a trapezoidal channel. Plot the ratio R/y for $b=2$ m with side slope angles of 30° and 60° for 0.5 m $< y <$ 3 m.

11.2 A wave from a passing boat in a lake is observed to travel at 16 km/h. Determine the approximate water depth at this location.

11.3 A pebble is dropped into a stream of water that flows in a rectangular channel at 2 m depth. In one second, a ripple caused by the stone is carried 7 m downstream. What is the speed of the flowing water?

11.4 A pebble is dropped into a stream of water of uniform depth. A wave is observed to travel upstream 1.5 m in 1 s and 3.9 m downstream in the same time. Determine the flow speed and depth.

11.5 Solution of the complete differential equations for wave motion without surface tension shows that wave speed is given by

$$c=\sqrt{\frac{g\lambda}{2\pi}\tanh\left(\frac{2\pi y}{\lambda}\right)}$$

where λ is the wave wavelength and y the liquid depth. Show that when $\lambda/y \ll 1$, wave speed becomes proportional to $\sqrt{\lambda}$. In the limit as $\lambda/y \to \infty$, $c=\sqrt{gy}$. Determine the value of λ/y for which $c > 0.99\sqrt{gy}$.

11.6 Solution of the complete differential equations for wave motion in quiescent liquid, including the effects of surface tension, shows that wave speed is given by

$$c=\sqrt{\left(\frac{g\lambda}{2\pi}+\frac{2\pi\sigma}{\rho\lambda}\right)\tanh\left(\frac{2\pi y}{\lambda}\right)}$$

where λ is the wave wavelength, y the liquid depth, and σ the surface tension. Plot wave speed versus wavelength for the range 1 mm < λ < 100 mm for (a) water and (b) mercury. Assume $y=7$ mm for both liquids.

11.7 Surface waves are caused by a sharp object that just touches the free surface of a stream of flowing water, forming the wave pattern shown. The stream depth is 150 mm. Determine the flow speed and Froude number. Note that the wave travels at speed c (Eq. 11.6) normal to the wave front, as shown in the velocity diagram.

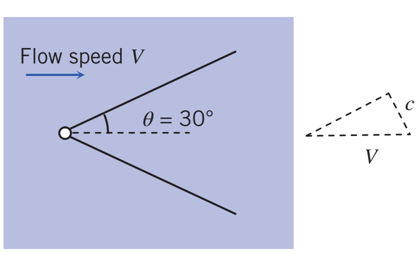

P11.7

11.8 A submerged body traveling horizontally beneath a liquid surface at a Froude number (based on body length) about 0.5 produces a strong surface wave pattern if submerged less than half its length. (The wave pattern of a surface ship also is pronounced at this Froude number.) On a log-log plot of speed versus body (or ship) length for 1 m/s $< V <$ 30 m/s and 1 m $< x <$ 300 m, plot the line $Fr=0.5$.

11.9 Water flows in a rectangular channel at a depth of 750 mm. If the flow speed is (a) 1 m/s and (b) 4 m/s, compute the corresponding Froude numbers.

11.10 A long rectangular channel 3 m wide is observed to have a wavy surface at a depth of about 1.8 m. Estimate the rate of discharge.

Energy Equation for Open-Channel Flows

11.11 For a rectangular channel of width $b=20$ m, construct a family of specific energy curves for $Q=0$, 25, 75, 125, and 200 m^3/s. What are the minimum specific energies for these curves?

11.12 A trapezoidal channel with a bottom width of 6 m, side slopes of 1 to 2, channel bottom slope of 0.0016, and a Manning's n of 0.025 carries a discharge of 11.3 m^3/s. Compute the critical depth and velocity of this channel.

11.13 A rectangular channel carries a discharge of 0.93 m^3/s per meter of width. Determine the minimum specific energy possible for this flow. Compute the corresponding flow depth and speed.

11.14 Flow in the channel of Problem 11.13 ($E_{\text{min}}=0.66$ m) is to be at twice the minimum specific energy. Compute the alternate depths for this E.

11.15 For a channel of nonrectangular cross section, critical depth occurs at minimum specific energy. Obtain a general equation for critical depth in a trapezoidal section in terms of Q, g, b, and α. It will be implicit in y_c!

11.16 Water flows at 8.5 m^3/s in a trapezoidal channel with bottom width of 2.4 m. The sides are sloped at 2:1. Find the critical depth for this channel.

Localized Effects of Area Change (Frictionless Flow)

11.17 Consider the Venturi flume shown. The bed is horizontal, and flow may be considered frictionless. The upstream depth is 0.3 mm, and the downstream depth is 0.22 m. The upstream breadth is 0.6 m, and the breadth of the throat is 0.3 m. Estimate the flow rate through the flume.

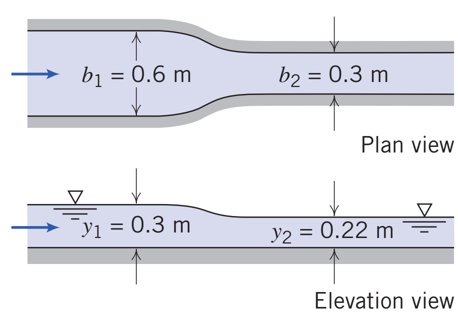

P11.17

11.18 A rectangular channel 3 m wide carries 2.83 m^3/s on a horizontal bed at 0.3 m depth. A smooth bump across the channel rises 10 cm. above the channel bottom. Find the elevation of the liquid free surface above the bump.

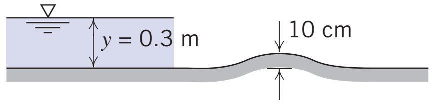

P11.18

11.19 A rectangular channel 3 m wide carries a discharge of 0.57 m^3/s at 0.27 m depth. A smooth bump 0.06 m high is placed on the floor of the channel. Estimate the local change in flow depth caused by the bump.

11.20 At a section of a 3 m-wide rectangular channel, the depth is 0.09 m for a discharge of 0.57 m^3/s. A smooth bump 0.03 m high is placed on the floor of the channel. Determine the local change in flow depth caused by the bump.

11.21 Water, at 0.9 m/s and 0.6 m depth, approaches a smooth rise in a wide channel. Estimate the stream depth after the 0.15 m rise.

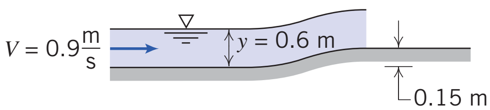

P11.21

11.22 Water issues from a sluice gate at 1.25 m depth. The discharge per unit width is 10 m^3/s/m. Estimate the water level far upstream where the flow speed is negligible. Calculate the maximum rate of flow per unit width that could be delivered through the sluice gate.

11.23 A horizontal rectangular channel 0.9 m wide contains a sluice gate. Upstream of the gate the depth is 1.8 m; the depth downstream is 0.27 m. Estimate the volume flow rate in the channel.

11.24 Flow through a sluice gate is shown. Estimate the water depth and velocity after the gate (well before the hydraulic jump).

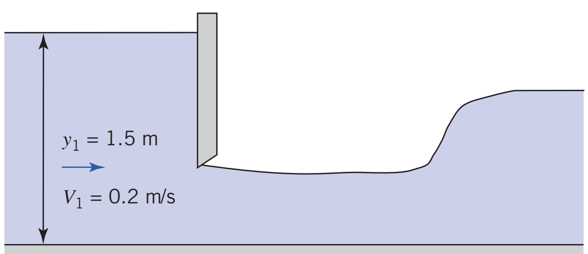

P11.24, P11.30

11.25 Rework Example 11.4 for a 350-mm-high bump and a side wall constriction that reduces the channel width to 1.5 m.

The Hydraulic Jump

11.26 Find the rate at which energy is being consumed (kW) by the hydraulic jump of Example 11.5. Is this sufficient to produce a significant temperature rise in the water?

11.27 A wide channel carries 10 m^3/s per foot of width at a depth of 1 m at the toe of a hydraulic jump. Determine the depth of the jump and the head loss across it.

11.28 A hydraulic jump occurs in a rectangular channel. The flow rate is 6.5 m^3/s, and the depth before the jump is 0.4 m. Determine the depth behind the jump and the head loss, if the channel is 1 m wide.

11.29 The hydraulic jump may be used as a crude flow meter. Suppose that in a horizontal rectangular channel 1.5 m wide the observed depths before and after a hydraulic jump are 0.2 and 0.9 m. Find the rate of flow and the head loss.

11.30 Estimate the depth of water before and after the jump for the hydraulic jump downstream of the sluice gate of Fig. P11.24.

11.31 A tidal bore (an abrupt translating wave or moving hydraulic jump) often forms when the tide flows into the wide estuary of a river. In one case, a bore is observed to have a height of 3.6 m above the undisturbed level of the river that is 2.4 m deep. The bore travels upstream at $V_{bore} = 28.97$ km/h. Determine the approximate speed V_r of the current of the undisturbed river.

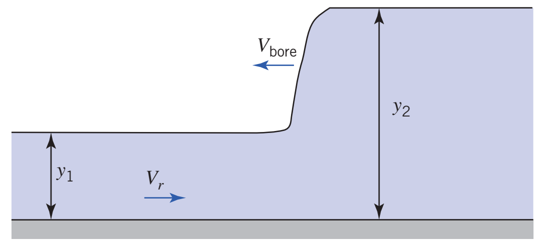

P11.31

Uniform Flow

11.32 Determine the uniform flow depth in a trapezoidal channel with a bottom width of 2.4 m and side slopes of 1 vertical to 2 horizontal. The discharge is 2.8 m^3/s. Manning's roughness factor is 0.015 and the channel bottom slope is 0.0004.

11.33 Determine the uniform flow depth in a trapezoidal channel with a bottom width of 2.5 m and side slopes of 1 vertical to 2 horizontal with a discharge of 3 m^3/s. The slope is 0.0004 and Manning's roughness factor is 0.015.

11.34 A rectangular flume built of concrete, with 1 m per 1000 m slope, is 1.8 m wide. Water flows at a normal depth of 0.9 m. Compute the discharge.

11.35 A rectangular flume built of timber is 0.9 m wide. The flume is to handle a flow of 2.55 m^3/s at a normal depth of 1.8 m. Determine the slope required.

11.36 Water flows in a trapezoidal channel at a normal depth of 1.2 m. The bottom width is 2.4 m and the sides slope at 1:1 (45°). The flow rate is 7.1 m^3/s. The channel is excavated from bare soil. Find the bed slope.

11.37 A semicircular trough of corrugated steel, with diameter $D = 1$ m, carries water at depth $y = 0.25$ m. The slope is 0.01. Find the discharge.

11.38 The flume of Problem 11.34 is fitted with a new plastic film liner ($n = 0.010$). Find the new depth of flow if the discharge remains constant at 2.42 m^3/s.

11.39 Consider a symmetric open channel of triangular cross section. Show that for a given flow area, the wetted perimeter is minimized when the sides meet at a right angle.

11.40 Compute the normal depth and velocity of the channel of Problem 11.12.

11.41 Determine the cross section of the greatest hydraulic efficiency for a trapezoidal channel with side slope of 1 vertical to 2 horizontal if the design discharge is 250 m^3/s. The channel slope is 0.001 and Manning's roughness factor is 0.020.

11.42 For a trapezoidal-shaped channel ($n = 0.014$ and slope $S_b = 0.0002$ with a 6-m bottom width and side slopes of 1 vertical to 1.5 horizontal), determine the normal depth for a discharge of 28.3 m^3/s.

11.43 Show that the best hydraulic trapezoidal section is one-half of a hexagon.

11.44 Consider a 2.45-m-wide rectangular channel with a bed slope of 0.0004 and a Manning's roughness factor of 0.015. A weir is placed in the channel, and the depth upstream of the weir is 1.52 m for a discharge of 5.66 m^3/s. Determine whether a hydraulic jump forms upstream of the weir.

11.45 An above-ground rectangular flume is to be constructed of timber. For a drop of 1.9 m/km, what will be the depth and width for the most economical flume if it is to discharge 1.1 m^3/s?

11.46 Consider flow in a rectangular channel. Show that, for flow at critical depth and optimum aspect ratio ($b = 2y$), the volume flow rate and bed slope are given by the expressions:

$$Q = 62.6 y_c^{5/2} \text{ and } S_c = 24.7 \frac{n^2}{y_c^{1/3}}$$

11.47 A trapezoidal canal lined with brick has side slopes of 2:1 and bottom width of 3 m. It carries 17 m^3/s at critical speed. Determine the critical slope (the slope at which the depth is critical).

11.48 A wide flat unfinished concrete channel discharges water at 1.9 m^3/s per meter of width. Find the critical slope (the slope at which depth is critical).

11.49 An optimum rectangular storm sewer channel made of unfinished concrete is to be designed to carry a maximum flow rate of 2.83 m^3/s, at which the flow is at critical condition. Determine the channel width and slope.

Discharge Measurement

11.50 The crest of a broad-crested weir is 0.3 m below the level of an upstream reservoir, where the water depth is 2.4 m. For $C_w \approx 3.4$, what is the maximum flow rate per unit width that could pass over the weir?

11.51 A rectangular, sharp-crested weir with end contraction is 1.6 m long. How high should it be placed in a channel to maintain an upstream depth of 2.5 m for 0.5 m^3/s flow rate?

11.52 For a sharp-crested suppressed weir ($C_w \approx 3.33$) of length $b = 2.4$ m, $P = 0.6$ m, and $H = 0.3$ m, determine the discharge over the weir. Neglect the velocity of approach head.

11.53 Determine the head on a 60° V-notch weir for a discharge of 150 L/s. Take $C_d \approx 0.58$.

11.54 The head on a 90° V-notch weir is 0.45 m. Determine the discharge.